cmgh
CELLULAR AND MOLECULAR GASTROENTEROLOGY AND HEPATOLOGY

ORIGINAL RESEARCH

The Fragile X Mental Retardation Protein Regulates RIP1K and Colorectal Cancer Resistance to Necroptosis

Antonio Di Grazia,[1] Irene Marafini,[1] Giorgia Pedini,[2] Davide Di Fusco,[1] Federica Laudisi,[1] Vincenzo Dinallo,[1] Eleonora Rosina,[2] Carmine Stolfi,[1] Eleonora Franzè,[1] Pierpaolo Sileri,[3] Giuseppe Sica,[3] Giovanni Monteleone,[1] Claudia Bagni,[2,4] and Ivan Monteleone[2]

[1]Department of Systems Medicine, University of Rome 'Tor Vergata', Rome, Italy; [2]Department of Biomedicine and Prevention, University of Rome 'Tor Vergata', Rome, Italy; [3]Department of Surgery, University of 'Tor Vergata', Rome, Italy; and [4]Department of Fundamental Neurosciences, University of Lausanne, Lausanne, Switzerland

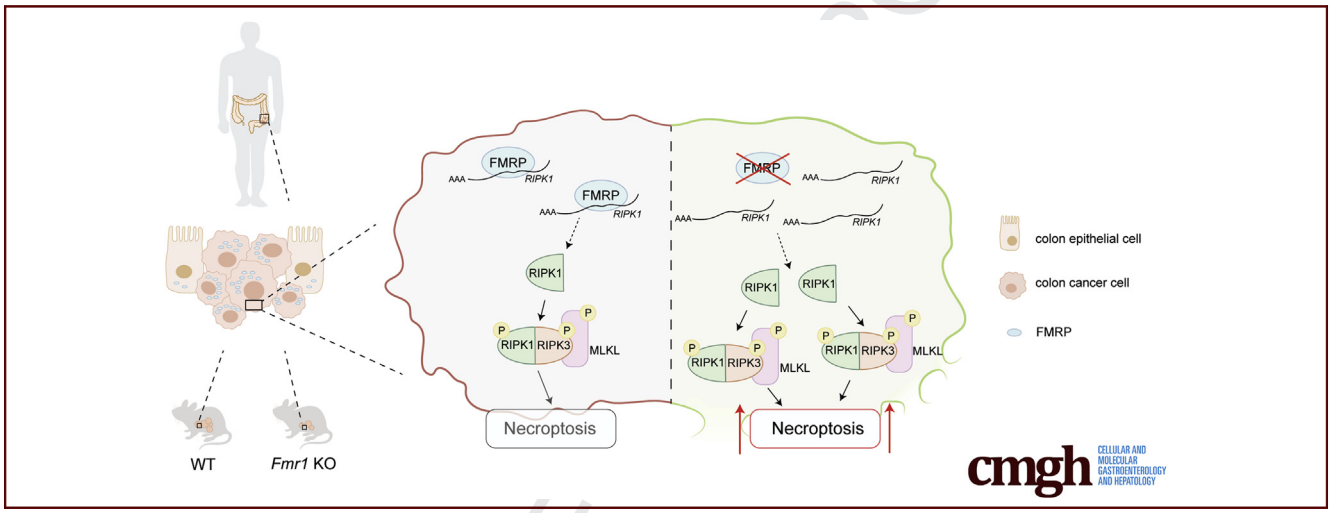

SUMMARY

The identification of a specific target as FMRP that could control directly the necroptosis pathway represents a novel attractive strategy to overcoming programmed cell death resistance in CRC.

BACKGROUND & AIMS: The fragile X mental retardation protein (FMRP) affects multiple steps of the mRNA metabolism during brain development and in different neoplastic processes. However, the contribution of FMRP in colon carcinogenesis has not been investigated.

METHODS: FMRP transcripts and proteins expression were analyzed in human colon samples derived from patients with sporadic colorectal cancer (CRC) and healthy subjects. We used a well-established mouse model of sporadic CRC induced by azoxymethane to determine the possible role of FMRP in CRC. To address whether FMRP controls cancer cell survival, we analyzed cell death pathway in CRC human epithelial cell lines and in patient-derived colon cancer organoid in presence or absence of a specific FMRP antisense oligonucleotide or siRNA.

RESULTS: We document a significant increase of FMRP in human CRC relative to non-tumor tissues. Next, using an inducible mouse model of CRC, we observed a reduction of colonic tumor incidence and size in the *Fmr1* knockout mice. The abrogation of FMRP induced spontaneous cell death in human CRC cell lines activating the necroptotic pathway. Indeed, specific immunoprecipitation experiments on human cell lines and CRC samples indicate that FMRP binds receptor-interacting protein kinase 1 (*RIPK1*) mRNA, suggesting that FMRP acts as a master regulator of necroptosis pathway through the surveillance of *RIPK1* mRNA metabolism. Treatment of human CRC cell lines and patient-derived colon cancer organoids with the *FMR1* antisense results in up-regulation of RIPK1, which drives the CRC human cell toward the necroptosis.

CONCLUSIONS: Altogether, these data support a role for FMRP in sustaining colon tumorigenesis controlling the RIPK1 expression and ultimately abrogating the activation of the necroptotic pathway. *(Cell Mol Gastroenterol Hepatol 2020;■:■–■; https://doi.org/10.1016/j.jcmgh.2020.10.009)*

Keywords: Colorectal Cancer; FMRP; Necroptosis; RIPK.

Colorectal cancer (CRC) is one of the most common cancers worldwide, causing half-million deaths every year.[1] CRC develops in a stepwise manner from normal mucosa to adenomatous polyps to carcinoma, a

complex and multistage process characterized by accumulation of genetic changes, each conferring a selective growth advantage to tumor cells.[2] These changes ultimately result in uncontrolled cell growth, resistance to cell death, and clonal tumor development.[2] These mechanisms are dictated by alterations of oncogenic and/or tumor-suppressive signaling pathways responsible for the progression from normal mucosa to adenomatous polyp and then to carcinoma.[2] During these sequential events driving toward the neoplastic phenotype, genetic and epigenetic changes that disrupt the balance between cell proliferation and cell death are crucial.[2]

In addition to transcriptional level, the oncogenic and/or tumor-suppressive signaling are tightly regulated at post-transcriptional levels such as splicing, transport to the cytoplasm, turnover, storage, and translation, processes largely regulated by RNA-binding proteins (RBPs).[3] RBPs are particularly interesting in the context of cancer, because many cancer-related proteins are encoded by mRNAs whose expression levels are regulated by RBPs modulating both mRNA translation and turnover.[3] Recent studies demonstrated the key contribution of several RBPs in the control of intestinal epithelial cell homeostasis and in response to injury.[4] Among the different pathways involved in CRC, a series of evidence highlights that colon tumor cells highjack posttranscriptional mechanisms that enable swift and robust adjustment of protein expression levels in response to intrinsic and extracellular signals, leading to cell adaptation to the local microenvironment.[5] Dysregulated RBPs influence the expression and function of pro-tumorigenic and tumor-suppressor proteins, among others.[5] Several studies have provided evidence that RBPs are abnormally expressed in cancer relative to adjacent normal tissues, and their expression correlates with patients' prognosis.[6,7] The fragile X mental retardation protein (FMRP), a RBP involved in multiple steps of mRNA metabolism, is gaining a pivotal importance in controlling the development and growth of different types of human cancer.[8–10] Mutations or absence of FMRP cause fragile X syndrome (FXS), the most frequent form of inherited intellectual disability in humans.[11] In the brain, FMRP absence causes impaired structural and functional synaptic plasticity due to defects in locally synthesized proteins, cytoskeletal organization, and receptor mobility.[11] FMRP can act as a negative regulator of translation and, in addition, modulates the stability, transport, or editing of the mRNAs depending on the identity of the target mRNA and the cellular context.[11,12] Of note, several of the brain-identified FMRP-regulated mRNAs are involved in mechanisms controlling cancer progression and metastasis formation.[13]

In cancer tissues, FMRP is highly expressed in triple negative breast cancers and in aggressive melanoma progression.[14,15] In addition, a decreased risk of different cancer types has been reported in a Danish and British cohort of patients with FXS, and a case report showed an unusual low growth of glioblastoma in a boy with FXS.[16,17] Finally, FMRP promotes astrocytoma proliferation via the MEK/ERK signaling pathway.[10] Overall, these data suggest that specific FMRP-regulated mechanisms might affect malignant transformation.

In this study, we assessed the role of FMRP in human sporadic CRC by using human and mouse models. We show that the absence of FMRP is protective toward cancer progression and identified the underlying molecular mechanism based on the control of the receptor-interacting serine/threonine-protein kinase 1 (RIPK1), a key mediator of the necroptosis pathway.

Results

FMRP Is Up-regulated in Human CRC Tissues and Cell Lines

To address the question whether FMRP is involved in disease survival of patients with CRC, different publicly online available datasets were screened for genetic alterations or aberrant protein expression levels of FMRP. *FMR1* mRNA and FMRP protein are highly expressed in different tissues and in cancer cell types (http://www.cbioportal.org/; https://www.proteinatlas.org/). The Kaplan-Meier analysis from the human protein atlas (https://www.proteinatlas.org/), consisting of 597 patients with CRC, showed a reduced disease-free survival in CRC patients with low expression of FMRP (5-year survival in high expression group, 69%; 5-year survival in low expression group, 59%). However, the analysis of the CRC available dataset on CBioPortal (http://www.cbioportal.org/; 3667 patients) reveals that patients with a nonfunctional or trunked FMRP proteins (49 patients) have a favorable outcome (5-year survival in mutated FMR1 gene group, 70%; 5-year survival in not mutated FMR1 gene group, 57%). Moreover, CRC available dataset on Cancer Genome Atlas (https://portal.gdc.cancer.gov/; 606 patients) reveals that patients with a mutation in the FMR1 gene (48 patients) have a favorable outcome (5-year survival in mutated FMR1 gene group, 73%; 5-year survival in not mutated FMR1 gene group, 62%). Although there are some discrepancies between protein expression and gene mutation of FMRP/*FMR1* and CRC survival, the absence of a functional FMRP seems to be protective in cancer. We examined *FMR1* mRNA and FMRP protein expression level in tumor and normal samples. *FMR1* mRNA expression was analyzed by real-time quantitative polymerase chain reaction (RT-qPCR) in tumor areas of human CRC samples (T) and in colonic samples derived from healthy mucosa of patients without cancer (NT). *FMR1* expression was higher in cancer samples with

Abbreviations used in this paper: **AnnV, annexin V; AOM, azoxymethane; CRC, colorectal cancer; CREB, cyclic adenosine monophosphate responsive element-binding protein; DAPI, 4′,6-diamidino-2-phenylindole; FMRP, fragile X mental retardation protein; FXS, fragile X syndrome; HRP, horseradish peroxidase; KO, knockout; MLKL, mixed lineage kinase domain-like; NT, colonic samples derived from healthy mucosa of patients without cancer; PARP-1, poly (ADP-ribose) polymerase; PI, propidium iodide; RBP, RNA-binding protein; RIPK1, receptor-interacting protein kinase 1; RT-qPCR, real-time quantitative polymerase chain reaction; SD, standard deviation; SEM, standard error of the mean; T, tumor areas of human CRC samples; TUNEL, deoxyuride-5′-triphosphate biotin nick end labeling.**

2352-345X
https://doi.org/10.1016/j.jcmgh.2020.10.009

respect to NT, which showed a relatively lower level of *FMR1* mRNA (Figure 1*A*). We also analyzed FMRP protein expression levels by Western blotting and immunohistochemistry. FMRP protein was significantly up-regulated in human CRC samples compared with NT (Figure 1*B* and *C*). FMRP was highly expressed in approximately 60% of colon cancer samples (T) analyzed compared with healthy subjects (NT). Moreover, the majority of patients with high-grade tumors revealed an overexpression of FMRP in CRC samples; however, because of the low number of human patients, the analysis did not reach statistical significance (Figure 2*A*). FMRP expression was also analyzed by Western blotting in protein extracts from 6 matched pairs of human CRC and adjacent tissues. FMRP was significantly increased in CRC samples, compared with non-tumor mucosa (Figure 2*B*). FMRP was also highly expressed in 2 colon cancer cell lines DLD-1 and HCT-116 when compared with the non-cancer colonic epithelial cell line HCEC-1ct (Figure 1*D* and *E*). These data show that *FMR1* mRNA and FMRP protein are overexpressed in colon cancer tissue.

CREB Controls FMRP Expression in Human CRC

FMRP expression is modulated by the transcription factor cyclic adenosine monophosphate responsive element-binding protein (CREB) pathways,[18] a protein closely associated with development and progression of human colon cancer.[19] *CREB* mRNA and protein were significantly increased in the areas of the colon tumor, similarly CREB activity (Figure 3*A* and *B*). The expression of the transcription factor Mef2, which is also involved in cancer and FMRP modulation, did not show any change (Figure 2*C* and *D*).[20] Furthermore, there is a clear direct relationship in individual samples between the expression of CREB and the amount of FMRP in CRC samples (Figure 3*C*). To investigate whether CREB levels were directly linked to FMRP levels in CRC, CREB expression was inhibited with a specific antisense oligonucleotide (ASc). In DLD-1 and HCT-116 cells *CREB* antisense oligonucleotide reduced CREB levels and showed a significant decrease of FMRP levels, whereas no effect was observed with the control oligonucleotide (Sc) (Figure 2*E*, Figure 3*D*). This finding suggests that in human CRC cells CREB positively controls FMRP expression consistent with previous studies and a CREB site on the *FMR1* gene promoter.[21,22]

Reduction of FMRP Results in a Better Outcome of CRC

To determine the possible role of FMRP in CRC, we used a well-established mouse model of sporadic CRC induced by azoxymethane (AOM).[23,24] Wild-type (WT) and *Fmr1* knockout (*Fmr1* KO) mice were injected intraperitoneally with AOM and monitored for tumor formation. Endoscopy performed on week 21 after the end of the AOM treatment showed that WT mice developed large tumors as previously reported.[24] In contrast, the number and size of the tumors generated in the *Fmr1* KO mice were significantly reduced (Figure 4*A* and *B*). These results were confirmed by direct assessment of tumors in mice killed on week 22. This difference in tumor size and number was accompanied by a decrease of viability by 20% in AOM WT mice compared with all the other groups as shown in the survival curve (Figure 4*C*). Histologic evaluation showed that in the absence of AOM treatment, the cellular morphology and organization of FMRP–deficient mice colon were comparable with WT mice (data not shown). However, in AOM-treated mice, tumors excised at 22 weeks showed that WT mice developed well-differentiated tumors, whereas *Fmr1* KO animals had a preserved normal tissue architecture nearby dysplastic areas (Figure 4*D*). Consistent with the observations in human CRC samples, Western blotting analysis showed an increase of FMRP expression in the tumor areas of WT AOM-treated mice, compared with WT mice in the absence of AOM treatment (Figure 4*E*). To investigate whether the decreased tumorigenesis observed in the *Fmr1* KO animals on AOM treatment was due to either an increase of cell death or a decrease of tumor cell proliferation, we performed a deoxyuride-5′-triphosphate biotin nick end labeling (TUNEL) assay, and we evaluated the level of Ki67. In addition, we evaluated the expression of the active (cleaved form) poly (ADP-ribose) polymerase (PARP-1), a nuclear enzyme whose products are involved in cell death programs.[25] The AOM *Fmr1* KO mice showed an increased number of TUNEL-positive cells and an increased expression of cleaved PARP-1 compared with AOM WT mice (Figure 4*F* and *G*), whereas no differences were observed in the number of Ki67-positive cells (Figure 2). These observations indicate that FMRP could amplify the tumor resistance to cell death, raising the possibility that FMRP can play an important role in colon carcinogenesis.

FMRP Affects Survival in Human CRC Cells

To address whether FMRP controls cancer cell survival, we analyzed cell death in CRC human epithelial cell lines in presence or absence of FMRP. Treatment of DLD-1 and HCEC-1ct cells with a specific *FMR1* RNA antisense oligonucleotide (AS) but not with the sense oligonucleotide (S) significantly reduced FMRP expression (Figure 5*A*). DLD-1 cells treated with the *FMR1* AS showed an induced susceptibility to spontaneous cell death; in particular the majority of the DLD-1 cells appear AnnexinV (AnnV)+ or AnnV+ propidium iodide (PI)+, the typical flow cytometry stigmata of programmed cell death (Figure 5*A*). This effect was cancer cell type specific and did not occur in normal human epithelial colon cells HCEC-1ct (Figure 5*B*). Similar results were obtained silencing *FMR1* in DLD-1 cells by using independent approaches, namely a specific *FMR1* small interfering RNA (Figure 6*A*).

To dissect the molecular mechanism observed on *FMR1* AS oligonucleotide-induced cell death, we analyzed the activation of caspase 8 and caspase 3, which play a role in the initiation and execution of cell apoptosis.[26] Treatment of DLD-1 cells with *FMR1* AS oligonucleotide did not alter the percentage of activated caspase 3 or caspase 8 positive cells (Figure 7*A*). Staurosporin, a well-known inducer of apoptosis, significantly increased the percentage of activated caspase 3 positive cells (Figure 7*A*). Furthermore, a

pretreatment of cells with a pan-caspase inhibitor did not alter *FMR1* AS oligonucleotide-induced cell death (Figure 7*B*). In addition, the treatment of DLD-1 cells with *FMR1* AS oligonucleotide did not alter mitochondrial membrane potential, the expression of gasdermin D and glutathione peroxidase 4, two key molecules that regulate the pyroptosis or ferroptosis pathways, respectively (Figure 6*B* and *C*).

To verify whether *FMR1* AS oligonucleotide-induced cell death was secondary to cell growth arrest, we analyzed the

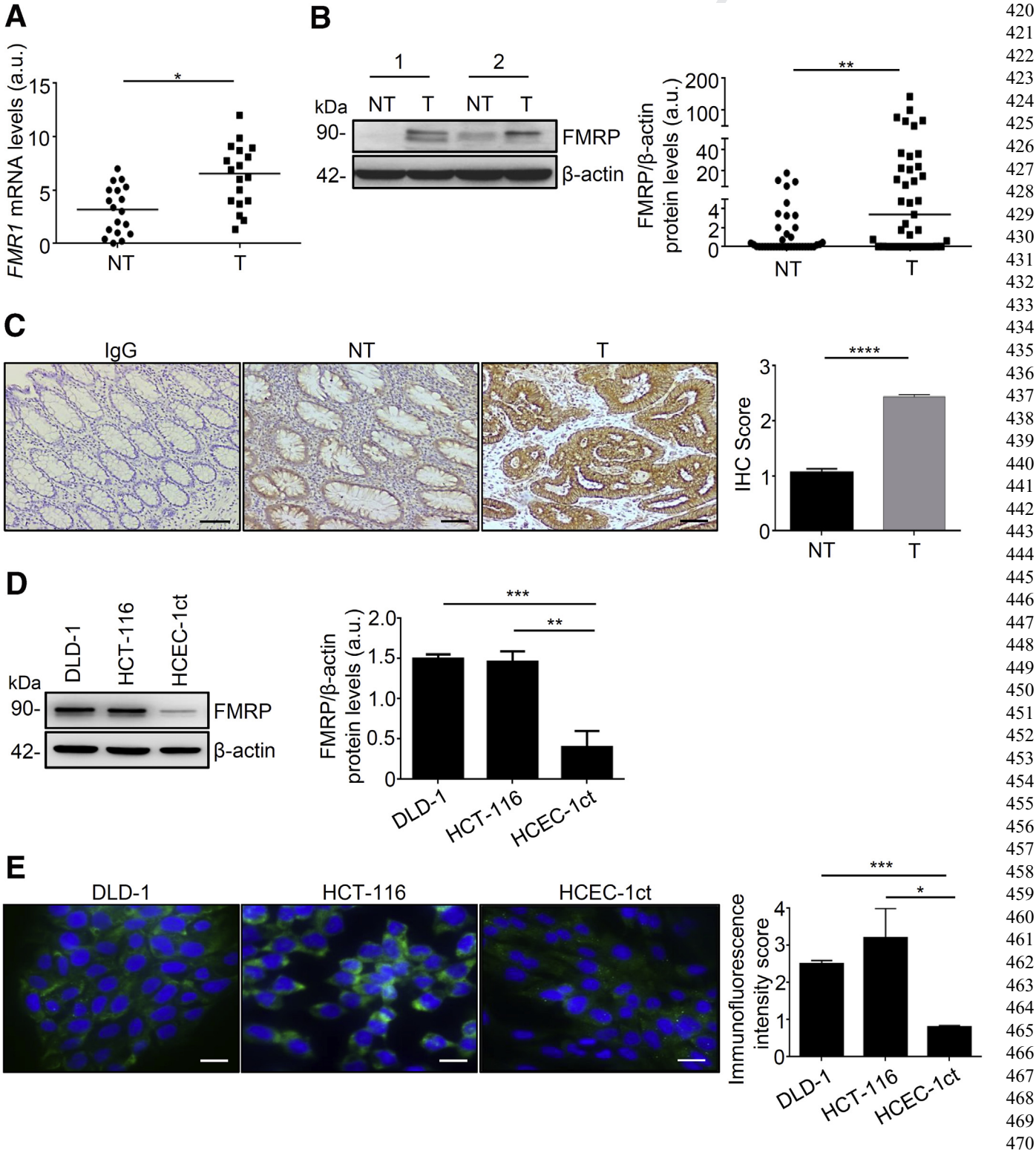

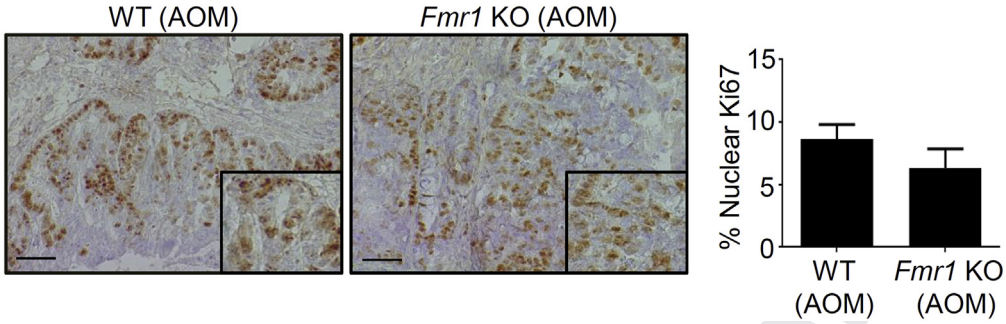

Figure 2. Representative Ki67 (G) staining of colonic sections from WT AOM and *Fmr1* KO AOM mice. *Right inset* indicates the % of Ki67+ cells (mean ± SD, n = 8 mice for *Fmr1* KO and 6 mice for WT group; WT AOM versus *Fmr1* KO AOM, $^{**}P < .01$). Statistical analysis of the data was performed using Mann-Whitney test.

cell cycle in DLD-1 cell lines. The *FMR1* AS oligonucleotide incubation did not affect cell cycle before the induction of cell death (Figure 7*C*). Altogether, these findings suggest that FMRP influences CRC cell death without affecting the apoptotic pathway or cell cycle.

FMRP Regulates the Necroptotic Pathway

Necroptosis is a regulated necrotic cell death modality in a caspase-independent manner and is mainly mediated by RIPK1, RIPK3, and mixed lineage kinase domain-like (MLKL).[27–29] This core complex, called the necrosome, mediates downstream executing molecules and events such as reactive oxygen species burst, plasma membrane permeabilization, and cytosolic adenosine triphosphate reduction that drives to the irreversible necroptosis-executing mechanisms.[30,31] Next we explored the possibility that the induced cell death in the absence of FMRP could be due to the activation of necroptosis pathway. We evaluated whether FMRP binds the mRNAs encoding the core components of the necroptosis complex, RIPK1 and RIPK3. FMRP was immunoprecipitated from human CRC samples and DLD-1 cell lines, and the association of candidate mRNAs tested by RT-qPCR (Figure 8*A* and *B*). We showed significant enrichment of *RIPK1* mRNA in the FMRP complex from human CRC tissues and DLD-1 cell lines, whereas *RIPK3* mRNA was not (Figure 8*A* and *B*); *β-actin*, *hypoxanthine phosphoribosyltransferase 1* (*HPRT1*), *vimentin,* and *E-cadherin* mRNAs were used as negative and positive controls, respectively.[15] These data suggest that FMRP binds *RIPK1* mRNA and thus possibly controls the fate of *RIPK1* mRNA, an initial core element of the necroptosis pathway. Although FMRP could act at the level of mRNA stability and/or mRNA translation, the stability of *RIPK1* mRNA seems not to be affected (data not shown).

FMRP Regulates Cell Death Modulating the RIPK/MLKL Pathway

To examine whether FMRP is responsible for inhibiting RIPK1 signaling in CRC, we explored RIPK1 expression in DLD-1 cell lines treated with *FMR1* AS oligonucleotide. Treatment of DLD-1 with the *FMR1* AS but not with the sense oligonucleotide inhibited FMRP expression (Figure 9*A*). Reduction of FMRP levels was associated with an increase in phosphorylation of RIPK1, RIPK3, and MLKL (Figure 9*A*). Of note, *FMR1* AS treatment led to a significant increase of RIPK1 protein and mRNA (Figure 9*A* and *B*). In the healthy colon cell line HCEC-1ct no changes in the expression/phosphorylation of RIPK1, RIPK3, and MLKL were observed on *FMR1* mRNA silencing (Figure 9*C*). Finally, we exploited the effect of *FMR1* mRNA silencing in patient-derived human colon

Figure 1. (*See previous page*). FMRP is overexpressed in human CRC and in CRC cell lines. (*A*) *FMR1* mRNA levels detected by RT-qPCR in colonic samples from 18 healthy subjects (NT) and tumor areas from 18 CRC patients (T); values were normalized to *β-actin* mRNA. *Each point* in the graph represents the value of *FMR1* mRNA in a single patient (NT versus T, $^{*}P < .05$). (*B*) *Left*, FMRP levels in representative images of Western blotting from colonic samples taken from 39 healthy subjects (NT) and 39 patients with CRC (T). β-actin was used as a loading control. *Right*, quantitative analysis of FMRP/β-actin protein ratio as measured by densitometry scanning of Western blots. *Each point* in the graph indicates the value of FMRP/β-actin in each patient (values are expressed in arbitrary units (a.u.); NT versus T, $^{*}P < .05$, $^{**}P < .01$). (*C*) Representative images of immunohistochemistry (IHC) and quantification for FMRP in colon sections taken from healthy subject (NT) and tumor areas of CRC patients (T) (n = 10). Immunoglobulin (Ig) G was used as a negative control ($^{****}P < .002$). *Scale bars*, 100 μm. (*D*) *Left*, FMRP levels in representative images of Western blotting from DLD-1, HCT-116 CRC cell lines and from healthy colon epithelial cell line HCEC-1ct. β-actin was used as a loading control. *Right*, quantitative analysis of FMRP/β-actin protein ratio (*right inset*) as measured by densitometry scanning of Western blots (values are expressed in arbitrary units (a.u.), mean ± SD of all experiments; DLD-1 versus HCEC-1ct, $^{***}P < .001$; HCT-116 versus HCEC-1ct, $^{**}P < .01$, n = 4). (*E*) Representative immunofluorescence of FMRP expression and quantification (*right panel*) in DLD-1, HCT-116, and HCEC-1ct cells, n = 5. DAPI (*blue*) and FMRP (*green*). (Mean ± SD of all experiments; DLD-1 versus HCEC-1ct, $^{***}P < .005$; HCT-116 versus HCEC-1ct, $^{*}P < .001$). *Scale bars*, 50 μm (the figure showed 50 mm). Statistical analysis of the data was performed using Student *t* test and the Mann-Whitney test.

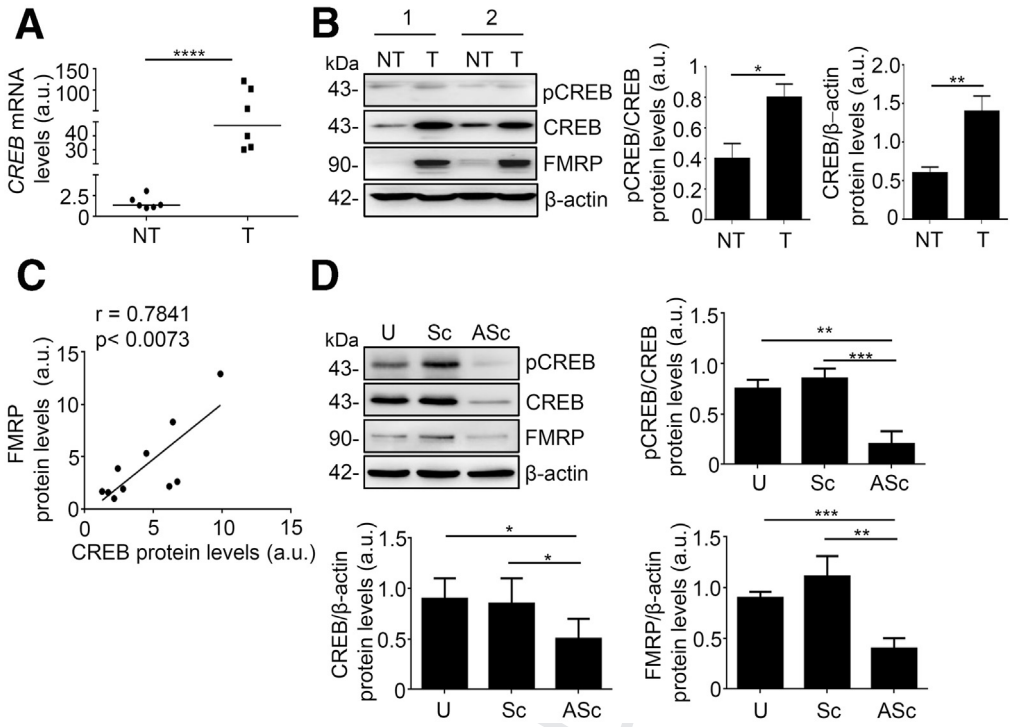

Figure 3. CREB controls FMRP expression in CRC cells. (*A*) *CREB* mRNA levels were evaluated by RT-qPCR in colonic samples from 6 healthy subjects (NT) and 6 patients with sporadic CRC (T, tumor areas); *β-actin* mRNA was used as normalizer (NT versus T, ****$P < .001$). (*B*) pCREB, CREB, and FMRP expression was evaluated by Western blotting in paired colonic samples from 10 healthy subjects and 10 patients with sporadic CRC. Technical duplicates were performed for each individual analyzed. pCREB/CREB and CREB/β-actin protein ratio was measured by densitometry scanning of Western blots (values are expressed in arbitrary units (a.u.), mean ± SD of all experiments; NT versus T, *$P < .05$, **$P < .01$). (*C*) Correlation between FMRP and CREB expression levels in mucosal samples from 10 CRC patients. Expression of FMRP is directly related to expression of CREB ($r = 0.7841$; $P < .0073$). (*D*) Representative Western blotting of DLD-1 cells unstimulated (U) or transfected with *CREB* sense (Sc) or *CREB* antisense (ASc) oligonucleotide for 48 hours. Histograms represent the quantification of pCREB/CREB, CREB/β-actin, and FMRP/β-actin protein ratio, as measured by densitometry scanning of Western blots (values are expressed in arbitrary units (a.u.), mean ± SD of 3 separate experiments; pCREB/β-actin: U-cells and Sc-transfected cells versus ASc-transfected cells, **$P < .01$, ***$P < .001$; CREB/β-actin: U-cells and Sc-transfected cells versus ASc-transfected cells, *$P < .05$; FMRP/β-actin: U-cells and Sc-transfected cells versus CREB ASc-transfected cells, **$P < .01$, ***$P < .001$). Statistical analysis of the data was performed using Student *t* test and Mann-Whitney test.

cancer organoids grown. Treatment of tumor organoids with *FMR1* AS significantly reduced FMRP expression, which led to a significant lower expression of RIPK1 (Figure 10*A*).

Next we evaluated the presence of *RIPK1* mRNA in the FMRP complex in the murine colon tissue. As shown in Figure 10*B*, a significant enrichment of *RIPK1* mRNA was detected after FMRP immunoprecipitation, suggesting that FMRP may regulate necroptosis in vivo during colon tumorigenesis. The analysis of the colon tumor area from the AOM *Fmr1* KO mice revealed an increased level of phosphorylated RIPK1, RIPK3, and MLKL (Figure 10*C*). To further evaluate whether FMRP-induced cell death was dependent from RIPK/MLKL complex activation, human CRC cell lines were incubated with RIPK1-specific inhibitor (NEC1) or MLKL-specific inhibitor (NSA). No difference in cell death was observed in DLD-1 cells incubated with *FMR1* AS oligonucleotide in presence of NEC1 or NSA inhibitors (Figure 9*D*). These data indicate *FMR1* AS oligonucleotide-induced cell death in CRC cells is due to the RIPK/MLKL intracellular signaling cascade.

Discussion

The intestinal epithelium illustrates a proliferation-differentiation gradient with a rapid renewal and turnover of cells.[32] The lifespan is based on a dynamic equilibrium that is regulated by several factors and that allows proliferation, migration, differentiation, and senescence of the cells.[32] This equilibrium can be disturbed during inflammation or injury that results from cellular stress mediated by infectious organisms, radiation, inflammatory disease, or harmful events.[2] These events trigger a rapid protective and regenerative response that is regulated by several intracellular and extracellular factors.[2] Prolonged injury together with genetic alterations can result in malignant transformation.[2] Similar process occurs in the development of CRC, which results from a combination of environmental, epigenetic, and genetic factors.[33] Compelling evidence indicates that CRC cells manifest enhanced activation of various intracellular signals that ultimately promote the expression of molecules involved in programmed cell death resistance or in cell growth.[27,34]

Among the factors that ensure the correct development of intestinal cells are RBPs. RBPs act in a rapid and efficient manner to alter gene expression, especially during changes in the microenvironment.[35] Increasing evidence indicates that the response and adaptation of intestinal epithelium to various types of injuries and to malignant transformation are mediated by RBPs.[35] A single RBP can bind to hundreds, if not thousands, of targets, and a combination of several RBPs interactions contribute to cellular identity in healthy condition, but also in cancer, RBPs regulate a number of mRNAs that encode for proteins involved in tumorigenesis.[5,36] In the specific case of CRC, several RBPs have been shown to be dysregulated and associated with survival rate of cancer patients.[35,37]

Of note, IMP1, CELF1, and HUR constitute a new set of regulatory RBPs, playing a role in intestinal homeostasis, adaptation to injury, and participation in malignant transformation.[35]

Here we show that FMRP expression is significantly increased in human CRC. Although the number of human cancer samples in this study does not allow us to analyze the relationship of FMRP expression with colon cancer patient outcome, previous observations indicate that FMRP levels are predictive of poor survival in multiple solid tumors.[14,15] The analysis of different cancer atlases (http://www.cbioportal.org/; https://www.proteinatlas.org/) revealed a high FMRP expression level in CRC tissues, further confirming and extending our observation. In addition, the available dataset on CRC (http://www.cbioportal.org/) reveals that patients with a mutation in the *FMR1* gene, encoding a nonfunctional or trunked FMRP proteins, have a favorable outcome (http://www.cbioportal.org/). Therefore, absence of a functional FMRP seems to be protective in cancer. However, analysis on public dataset of human protein atlas (https://www.proteinatlas.org/) showed a reduced disease-free survival in CRC patients with low expression of FMRP. Therefore, the analysis of different datasets showed some discrepancies about protection vs risk, suggesting that further analyses on a larger cohort of patients with CRC are required to evaluate whether FMRP levels correlate with prognostic indicators of aggressive CRC, metastases probability, and response to cancer therapies.

The expression of the *FMR1* gene is regulated at multiple levels, first among all by transcription factors,[21,38] and for example, the *FMR1* gene contains a CREB binding site.[21] Previous studies indicate that CREB affects colonic tumorigenesis, and neoplastic progression and suppression of CREB activity in cancer cells may also have a therapeutic effect.[19] Our data indicate that the transcription factor CREB, overexpressed in human CRC, controls positively FMRP expression in human colon cancer cells.

Using a well-established mouse model of CRC, we show that FMRP controls colon cancer progression. In AOM-treated *Fmr1* KO mice, colonic tumor incidence and size were significantly reduced compared with WT mice. However, because FMRP is relatively ubiquitously expressed, we cannot exclude the possibility that the anti-cancer effect detected in the *Fmr1* KO mice is also partly due to a control of the function of other mucosal cell types (eg, immune cells). However, the colon tissue analysis revealed an increased presence of tumor cell death in *Fmr1 KO* mice, suggesting, as indicated by the in vitro experiments, that the pro-tumorigenic function of FMRP is linked to a control of epithelial cancer cells survival.

Resistance to cell death is a crucial hallmark acquired during cancer progression, and a better understanding of deregulated pathways affecting cell death led to the development of therapeutic strategies that have been used with some success in CRC patients.[34] In normal tissues, programmed cell death plays a pivotal role in the development and maintenance of tissue homeostasis.[39] During the last 2 decades, several functional studies established that cell death serves as a natural barrier to cancer development.[40] CRC cells evolve a variety of strategies to limit or circumvent programmed cell death. Tumor cells may block apoptosis process by increasing expression of antiapoptotic regulators such as Bcl-2 and Bcl-xL, by down-regulating proapoptotic factors (Bax, Bim, Puma), or by short-circuiting the extrinsic ligand-induced death pathway.[2] RBPs can modulate the expression of genes implicated in cell survival,[35,36] and this prompted us to suppose that the pro-survival effect of FMRP could be controlled by inhibition of caspase/apoptotic mechanisms. However, the inhibition of caspase or cell cycle did not have an effect on cell death after a decrease of FMRP. In addition, inhibition of 2 key pathways of programmed cell death such as ferroptosis or pyroptosis also was not influenced by FMRP levels. These findings suggest that anti-survival effect of *FMR1* AS oligonucleotide is not due to the apoptotic, ferroptotic, pyroptotic mechanisms or secondary to cell cycle arrest. Necroptosis, a regulated cell death caspase-independent, could be an alternative way to eradicate resistant cell death in cancer cells.[27] Here we demonstrated that CRC cells incubated with *FMR1* AS oligonucleotide regain a normal activity of the necroptosis machinery that drives to programmed cell death (Figure S5). Specific immunoprecipitation experiments Q16 suggest that FMRP binds *RIPK1* mRNA, indicating that FMRP acts as a master regulator of the necroptosis pathway through the regulation of *RIPK1* mRNA metabolism at stability and/or mRNA translation levels. Of note, the application of high throughput approaches allowed the identification of hundreds of putative FMRP mRNA targets in brain (>1000) and in non-neuronal HEK293 cells (>6000).[41–44] FMRP has 4 RNA-binding domains: the Tudor domains and the K homology domains in the N-terminus region, 2 additional K homology domains in the central region, and in the C-terminal region of FMRP, an RGG box crucial for the interaction with some mRNAs containing a G-quartet structure.[45,46] So far, FMRP can bind mRNAs directly or indirectly via different types of sequences/structures.[47] In this study we provide for the first time the presence of *RIPK1* mRNA in the FMRP complex, indicating that FMRP could regulate its metabolism. Interestingly, using an available G-quadruplex prediction approach, namely G4CatchAll, we found 4 putative G-quadruplex structures in the *RIPK1* mRNA that represent a possible FMRP binding site. Although this is a predictive approach, the data are

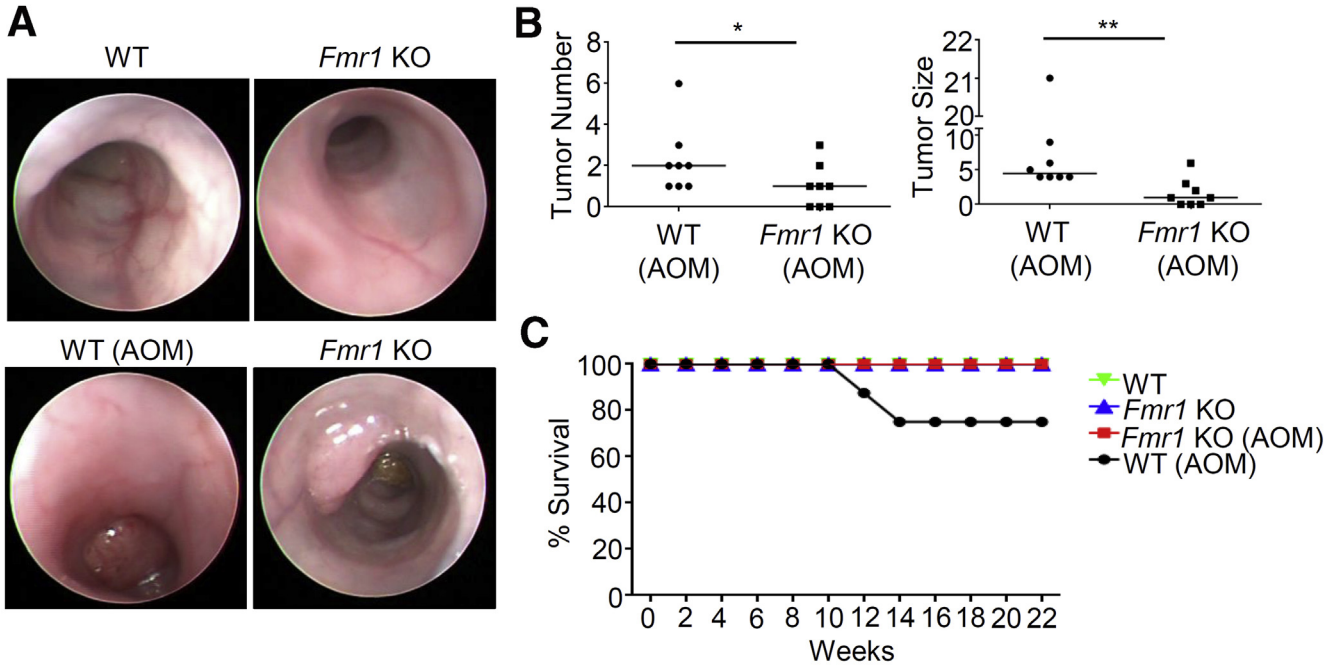
A
WT
Fmr1 KO
WT (AOM)
Fmr1 KO
B
Tumor Number
*
WT (AOM)
Fmr1 KO (AOM)
Tumor Size
**
WT (AOM)
Fmr1 KO (AOM)
C
% Survival
Weeks
WT
Fmr1 KO
Fmr1 KO (AOM)
WT (AOM)

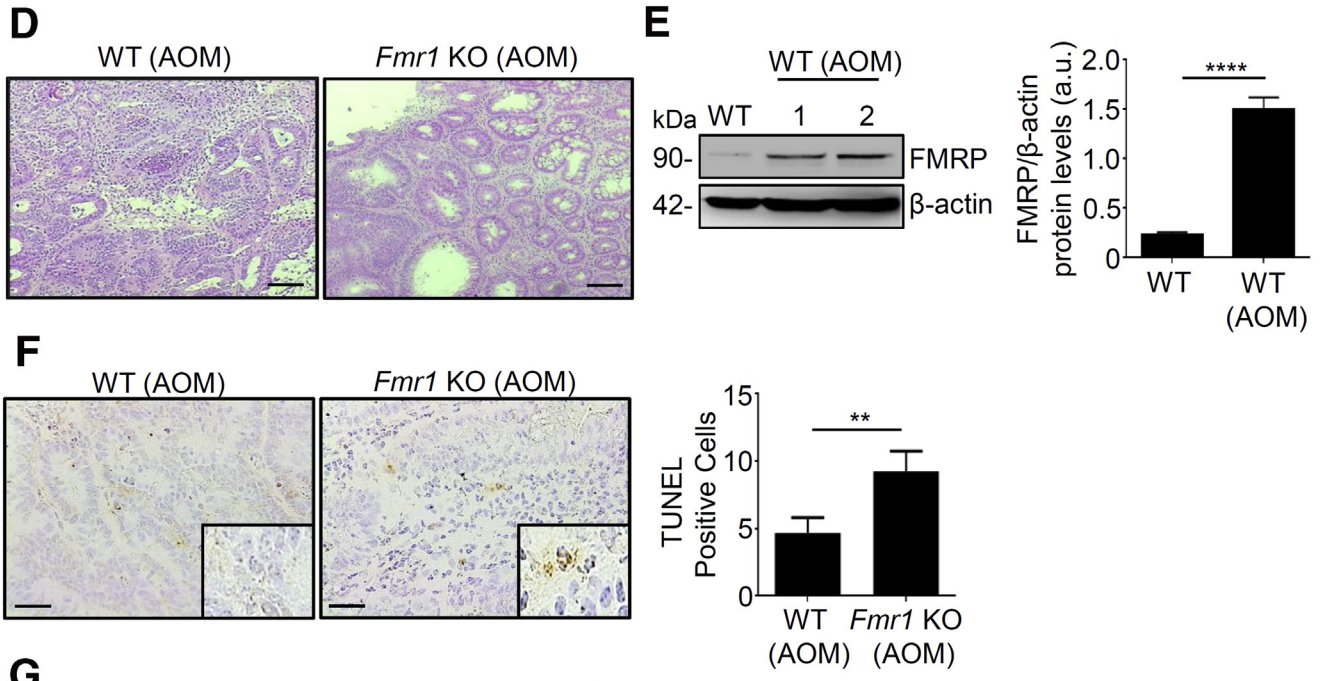
D
WT (AOM)
Fmr1 KO (AOM)
E
WT (AOM)
kDa WT 1 2
90-
FMRP
42-
β-actin
FMRP/β-actin protein levels (a.u.)
****
WT
WT (AOM)
F
WT (AOM)
Fmr1 KO (AOM)
TUNEL Positive Cells
**
WT (AOM)
Fmr1 KO (AOM)

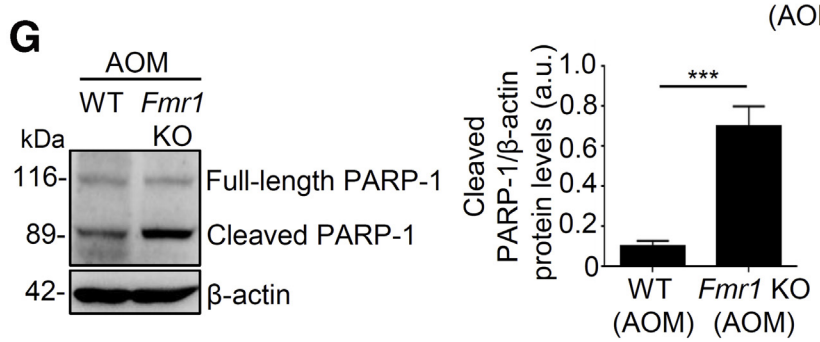
G
AOM
WT
Fmr1 KO
kDa
116-
Full-length PARP-1
89-
Cleaved PARP-1
42-
β-actin
Cleaved PARP-1/β-actin protein levels (a.u.)
***
WT (AOM)
Fmr1 KO (AOM)

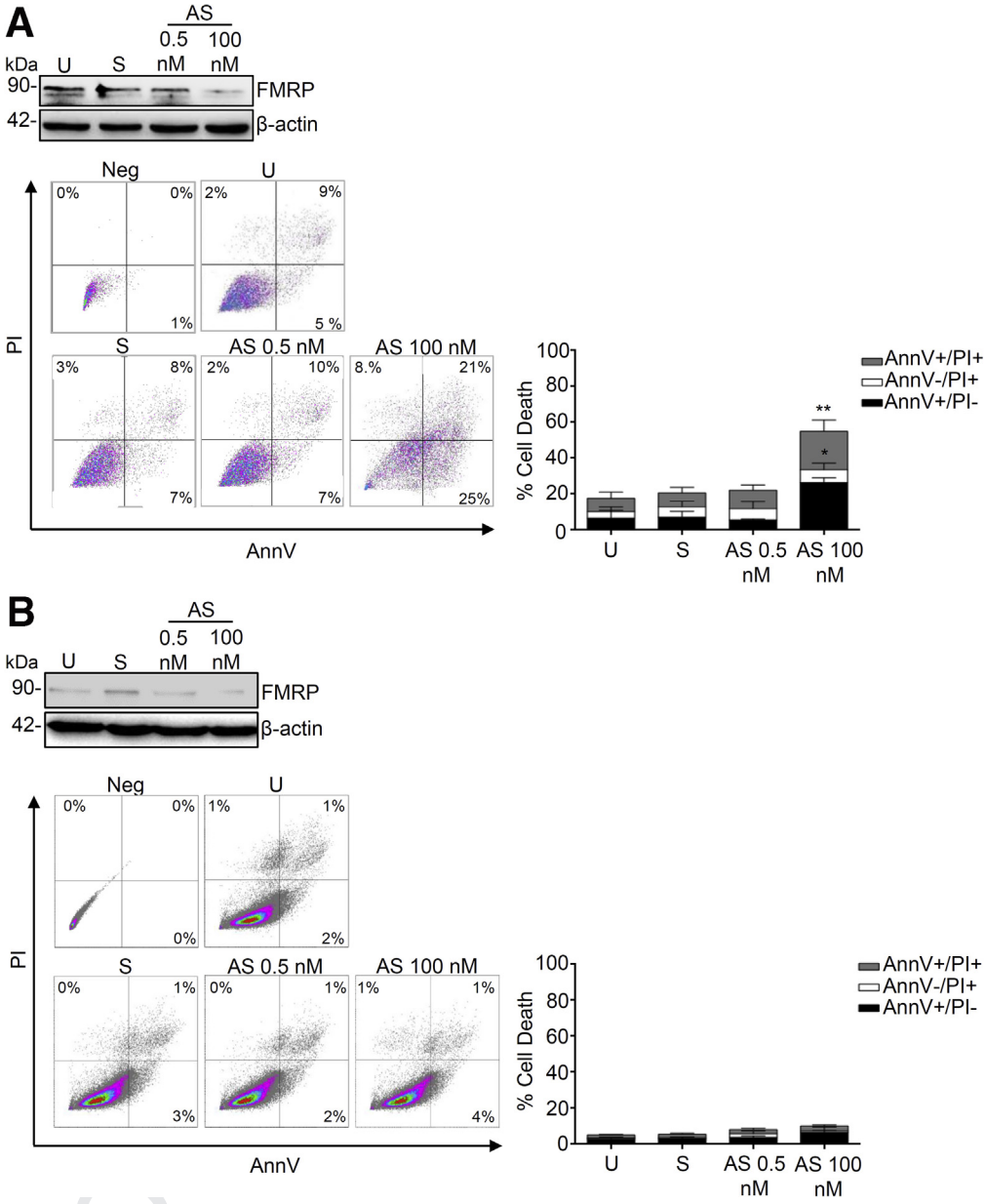

Figure 5. Knockdown of FMRP triggers cell death in CRC cell line. Representative blot showing FMRP expression in DLD-1 (*A*) or HCEC-1ct (*B*) cells unstimulated (U) or transfected with *FMR1* sense oligonucleotide (S) or *FMR1* antisense oligonucleotide (AS). Representative *dot blot* of AnnV and PI-positive DLD-1 or HCEC-1ct cells stimulated as indicated above (mean ± SEM, n = 5; U-cells and S-transfected cells versus AS-transfected cells, $*P < .05$, $**P < .01$). Statistical analysis of the data was performed using Mann-Whitney test.

Figure 4. (***See previous page***). ***Fmr1* KO mice present decreased colorectal tumorigenesis compared with WT.** (*A*) Representative images of endoscopic examination performed in WT and *Fmr1* KO mice at week 21 after injection with AOM. (*B*) Graphs show the number and size of colon tumors in WT and *Fmr1* KO AOM mice (WT AOM versus *Fmr1* KO AOM, $*P < .05$, $**P < .01$). (*C*) Kaplan-Meier curve of WT and *Fmr1* KO mice treated or not with AOM. (*D*) Representative staining with hematoxylin-eosin of tumor area from WT and *Fmr1* KO mice treated with AOM. *Scale bars*, 100 μm. (*E*) Representative Western blotting of FMRP expression in colon tissue from WT and WT mice treated with AOM. β-actin was used as a loading control. *Right*, quantitative analysis of FMRP/β-actin protein ratio (value is expressed in arbitrary units (a.u.), mean ± SD of all experiments; WT versus WT AOM, $****P < .0001$). (*F*) Representative images of TUNEL staining of colonic sections from WT AOM and *Fmr1* KO AOM mice. *Right inset* indicates the number of TUNEL+ cells (mean ± SD, n = 8 mice for each group; WT AOM versus *Fmr1* KO AOM, $**P < .01$). *Scale bars*, 50 μm. (*G*) Representative Western blotting of full-length and cleaved PARP-1 in colonic sections taken from WT AOM and *Fmr1* KO AOM mice. Data are representative of 3 experiments where similar results were obtained (n = 8 mice for each group). β-actin was used as loading control. *Right panel*, quantification of cleaved PARP-1/β-actin protein ratio (values are expressed in arbitrary units (a.u.), mean ± SD; WT AOM versus *Fmr1* KO AOM, $***P < .001$). Statistical analysis of the data was performed using Student *t* test and Mann-Whitney test. Survival analysis was performed using the Kaplan-Meier curve.

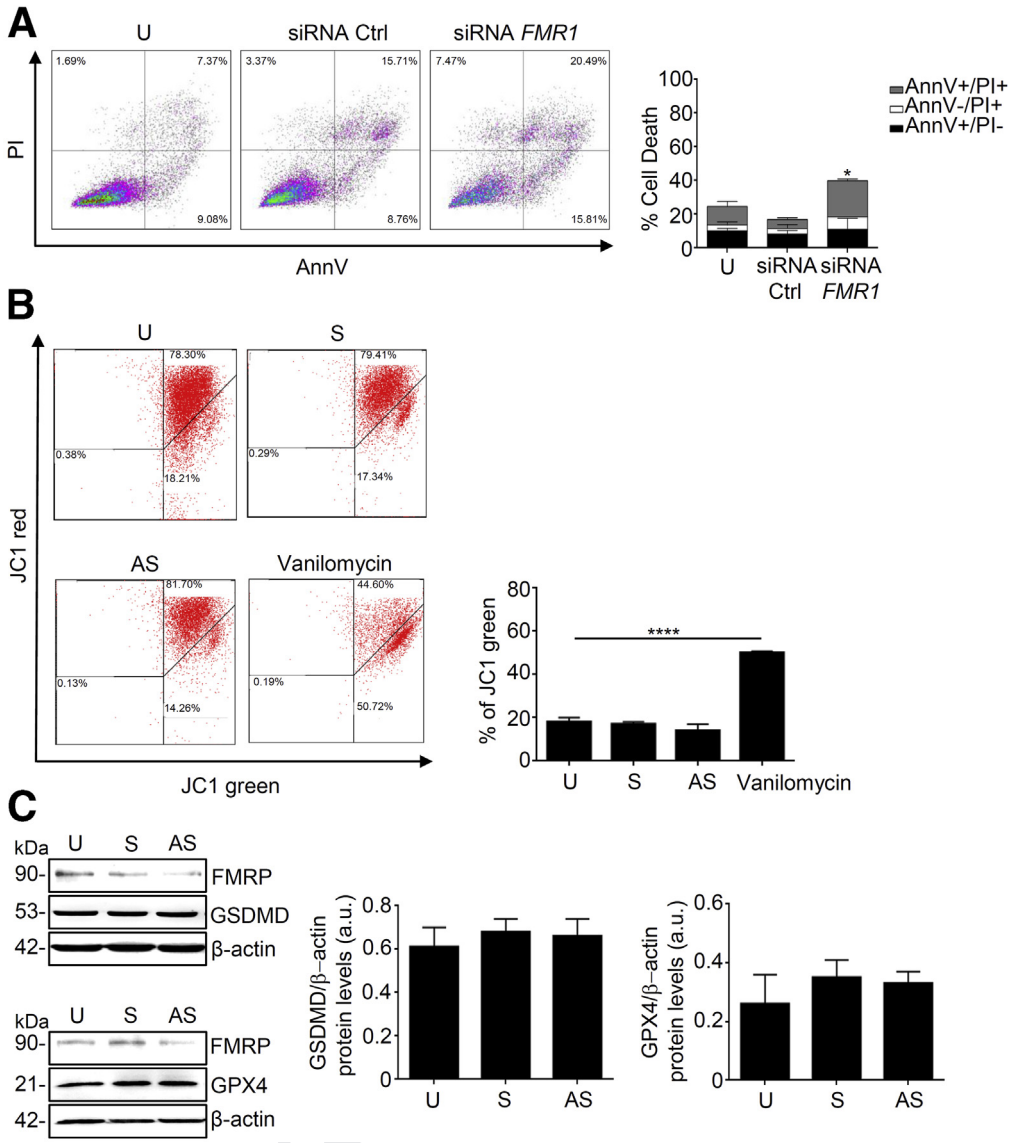

Figure 6. (*A*) DLD-1 cells unstimulated (U) or transfected with siCTRL or si*FMR1*. *Middle inset* shows representative *dot blot* of AnnV and PI-positive DLD-1 cells (mean ± SEM, n = 5; U-cells and siCTRL-transfected cells versus si*FMR1*-transfected cells, **P* < .05). (*B*) DLD-1 cells unstimulated (U) or transfected with *FMR1* sense (S) or *FMR1* antisense (AS) oligonucleotide or positive control valinomycin, stained with JC-1, and analyzed by flow cytometry. Mitochondrial membrane potential loss was observed as a decrease in JC-1 red fluorescence and an increase in JC-1 green fluorescence. *Inset* shows representative *dot blot* (mean ± SEM, n = 3; U cells, S cells and AS cells versus vanilomycin cells, ****P* < .001). (*C*) Representative Western blotting of GSDMD (*upper panel*) and GPX4 (*lower panel*) in DLD-1 cells unstimulated (U) or transfected with *FMR1* sense (S) or *FMR1* antisense (AS) oligonucleotide. β-actin was used as loading control. *Right panels*, quantification of GSDMD/β-actin (*upper panel*) and GPX4/ β-actin (lower panel) protein ratio (values are expressed in arbitrary units (a.u.), mean ± SD). Statistical analysis of the data was performed using Mann-Whitney test. GPX4, glutathione peroxidase 4; GSDMD, gasdermin D.

web 4C/FPO

promising, and future studies should further investigate whether FMRP could directly bind *RIPK1* mRNA.[48,49]

While our study was ongoing, Zhuang et al[50] showed that FMRP plays a central role in the inhibition of tumor necrosis factor (TNF)–mediated necroptosis during infection and liver disease. They demonstrated that FMRP is critically important for regulating key molecules in TNF receptor 1–dependent necroptosis including CYLD, c-FLIPS, and JNK, which contribute to prolonged RIPK1 expression and necrosome activation. Therefore, our findings together with the above-mentioned previous observations strengthen the hypothesis of targeting FMRP as an anti-cancer approach affecting both RIPK1 expression and the TNF-mediated necropoptosis.

Cancer cells are able to eradicate necroptosis machinery by down-regulation of the necroptotic core pathway and activate downstream executing molecules and events.[27,31] The identification of a master regulator such as FMRP could explain the molecular mechanism that allows to down-regulate RIPK1 expression in colon cancer. Moreover,

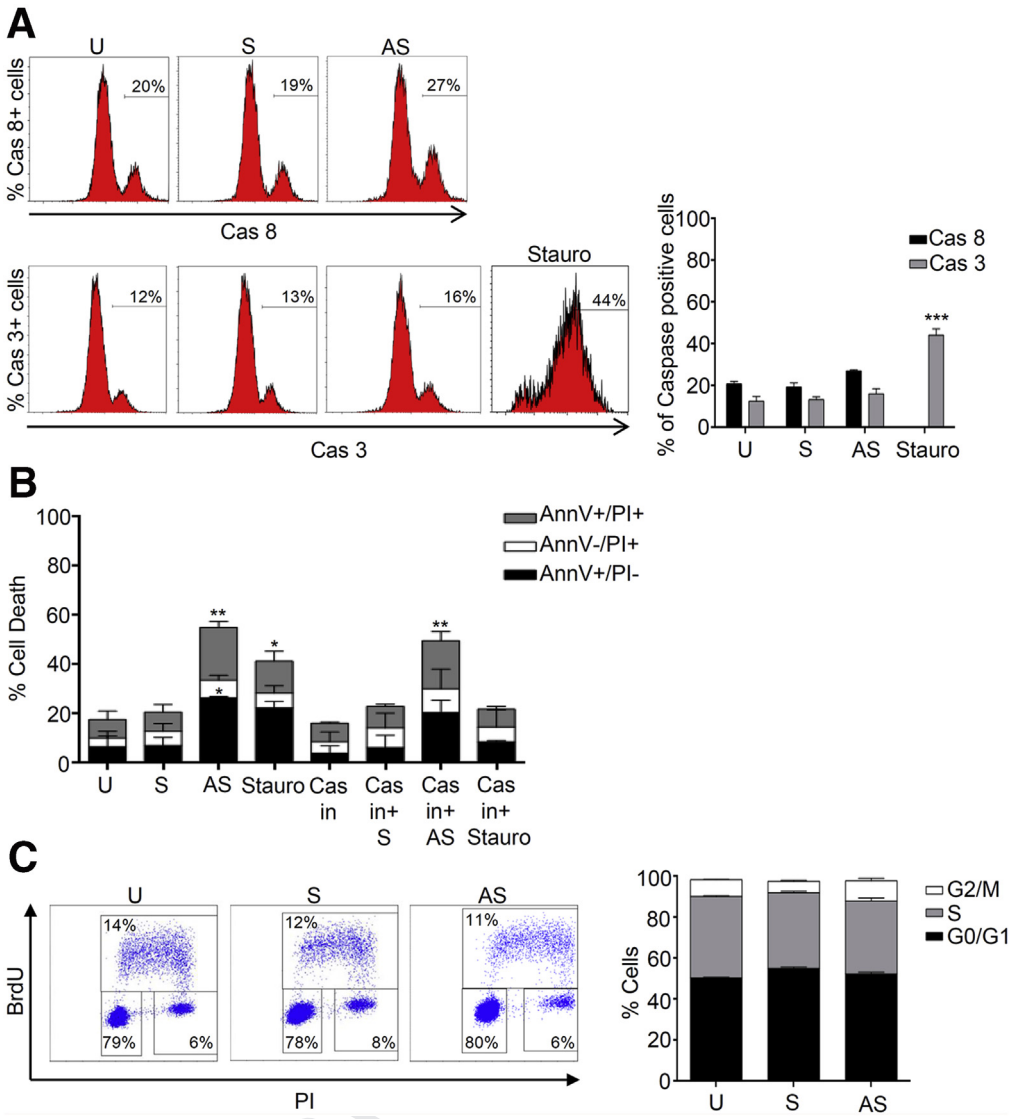

Figure 7. FMRP-triggered CRC cell death is caspase activation and cell cycle-independent. (*A*) Representative *dot blot* showing percentage of activated caspase 8 (Cas8) or activated caspase 3 (Cas3) positive DLD-1 cells unstimulated (U) or transfected with *FMR1* sense oligonucleotide (S) or antisense oligonucleotide (AS) for 36 hours. Staurosporin (Stauro) was used as positive control. *Right*, percentage of activated caspase3+ cells (*grey bar*) or activated caspase 8+ cells (*black bar*) measured by flow cytometry (mean ± SD, n = 3; U-cells, S-transfected cells, and AS-transfected cells versus Stauro-treated cells, ***$P < .001$). (*B*) Percentage of AnnV and/or PI-positive DLD-1 cells preincubated with pan-caspase inhibitor (Cas in) Z-VAD-FMK unstimulated (U) or transfected with *FMR1* sense oligonucleotide (S) or antisense oligonucleotide (AS) (mean ± SEM, n = 4; U-cells and S-transfected cells versus AS-transfected cells, **$P < .01$; U-cells, S-transfected cells versus Stauro, *$P < .05$). (*C*) *Left*, representative flow cytometric analysis of cell cycle progression in DLD-1 cells treated with *FMR1* sense (S) or antisense (AS) oligonucleotide. *Right*, percentages of cells in the different phases of cell cycle (mean ± SD, n = 3). Statistical analysis of the data was performed using Mann-Whitney test. BrdU, bromodeoxyuridine.

our results are consistent with the observation that overexpression of RIPK1 has been reported to suppress proliferation, migration, and invasion of human CRC cell lines.[51,52]

Proapoptotic therapy (eg, using cisplatin, carboplatin, paclitaxel, 5-fluorouracil, and gemcitabine), a major form of chemotherapy, is the principal method for cancer treatment, but the effectiveness of this therapy is limited by drug resistance and toxic effects. The discovery of necroptosis as an inducible, alternative form of programmed cell death has opened up novel and exciting perspectives to kill resistant cancer cells. Therefore, the control of necroptosis by defined signal transduction pathways offers the opportunity to target this cellular process for anti-cancer therapy.

Several strategies exist to trigger necroptosis in other human cancer types; the natural compound shikonin has been shown to bypass deficiencies in apoptosis pathways,[53] whereas Smac mimetics and the alkaloid staurosporine induce necroptosis in acute myeloid leukemia and different carcinoma cell lines.[54] Moreover, traditional chemotherapeutic or molecular targeted drugs approved for marketing

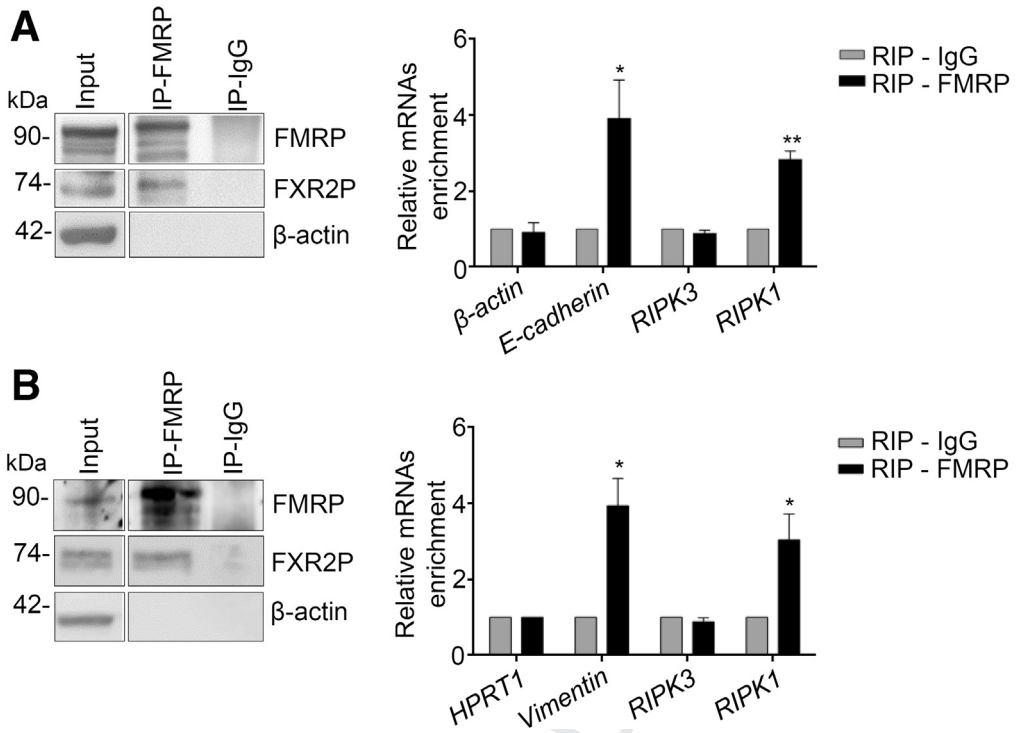

Figure 8. *RIPK1* mRNA is part of the FMRP complex. (*A*) *Left*, representative Western blotting of FMRP immunoprecipitation from colonic samples taken from 3 CRC patients. FXR2P, a well-known FMRP interactor, is detected as part of the FMRP complex; β-actin was used as a negative control. Input (1/20) of the total extract, FMRP immunoprecipitation (IP-FMRP), and mock immunoprecipitation (IP-IgG). *Right*, quantification by RT-qPCR of *β-actin, E-cadherin, RIPK3,* and *RIPK1* mRNAs. *β-actin* and *E-cadherin* mRNAs are negative and positive controls, respectively (mean ± SEM, n = 3; *E-cadherin*: IP-IgG versus IP-FMRP, $^{*}P < .05$; *RIPK1:* IP-IgG versus IP-FMRP, $^{**}P < .01$). (*B*) *Left*, representative Western blotting of FMRP immunoprecipitation from DLD-1 cell samples. FXR2P, a well-known FMRP interactor, is detected as part of the FMRP complex; β-actin is used as a negative control. Input (1/20) of the total extract, FMRP immunoprecipitation (IP-FMRP), and mock immunoprecipitation (IP-IgG). *Right*, quantification by RT-qPCR of *HPRT1*, *vimentin, RIPK3,* and *RIPK1* mRNAs in FMRP immunoprecipitation/total protein extracted from DLD-1 cells. *HPRT1* and *vimentin* mRNAs were used as negative and positive controls, respectively (mean ± SEM, n = 3; *vimentin*: IP-IgG versus IP-FMRP, $^{*}P < .05$; *RIPK1*: IP-IgG versus IP-FMRP, $^{*}P < .05$). Statistical analysis of the data was performed using Student *t* test.

or in clinical trials have been recently identified as cancer necroptosis inducers such as TRAIL, obatoclax, or 3-bromopyruvate plus chloroquine.[27,55,56] These drugs have been proven to be safe for human use, and induction of necroptosis in cancer cells does not have toxic effect in normal cells or lead to severe side effects in vivo. Therefore, the identification of a specific target such as FMRP that could control directly the necroptosis pathway could further enhance the specificity and selectivity of pro-necroptosis strategy. In conclusion, our data indicate that down-regulation of FMRP drives colon cancer cells to switch to necroptosis and represents a novel attractive strategy to overcoming programmed cell death resistance in CRC.

Methods

Patients and Human Samples

Samples of human CRC areas were derived from 67 patients who had undergone colonic resection for sporadic CRC, whereas healthy (normal) mucosa samples include colonic mucosal biopsy from 67 patients with irritable bowel syndrome from the University Hospital of Tor Vergata (Rome, Italy). FMRP and *FMR1* mRNA expression was evaluated by immunohistochemistry, Western blotting, and RT-qPCR. Paired tissue samples were derived from the tumoral area and the macroscopically unaffected, adjacent colonic mucosa of 6 patients who underwent colon resection for sporadic CRC at the Tor Vergata University Hospital (Rome, Italy) and used for FMRP expression by Western blotting. Patients with sporadic CRC received neither radiotherapy nor chemotherapy before surgery. Written informed consent was obtained from all patients. The study protocol was approved by the Tor Vergata University Hospital Review Board (protocol number 129/17).

Experimental Model of CRC

Mice were housed in a ventilated, temperature controlled (23°C) room with a 12-hour light/dark cycle. Starting at 6 weeks of age, male FVB.129P2 WT and *Fmr1* KO mice were injected with the alkylating agent AOM (10 mg/kg; Sigma-Aldrich, Milan, Italy) intraperitoneally once a week for 5 weeks to induce tumor formation.[23] Mice were

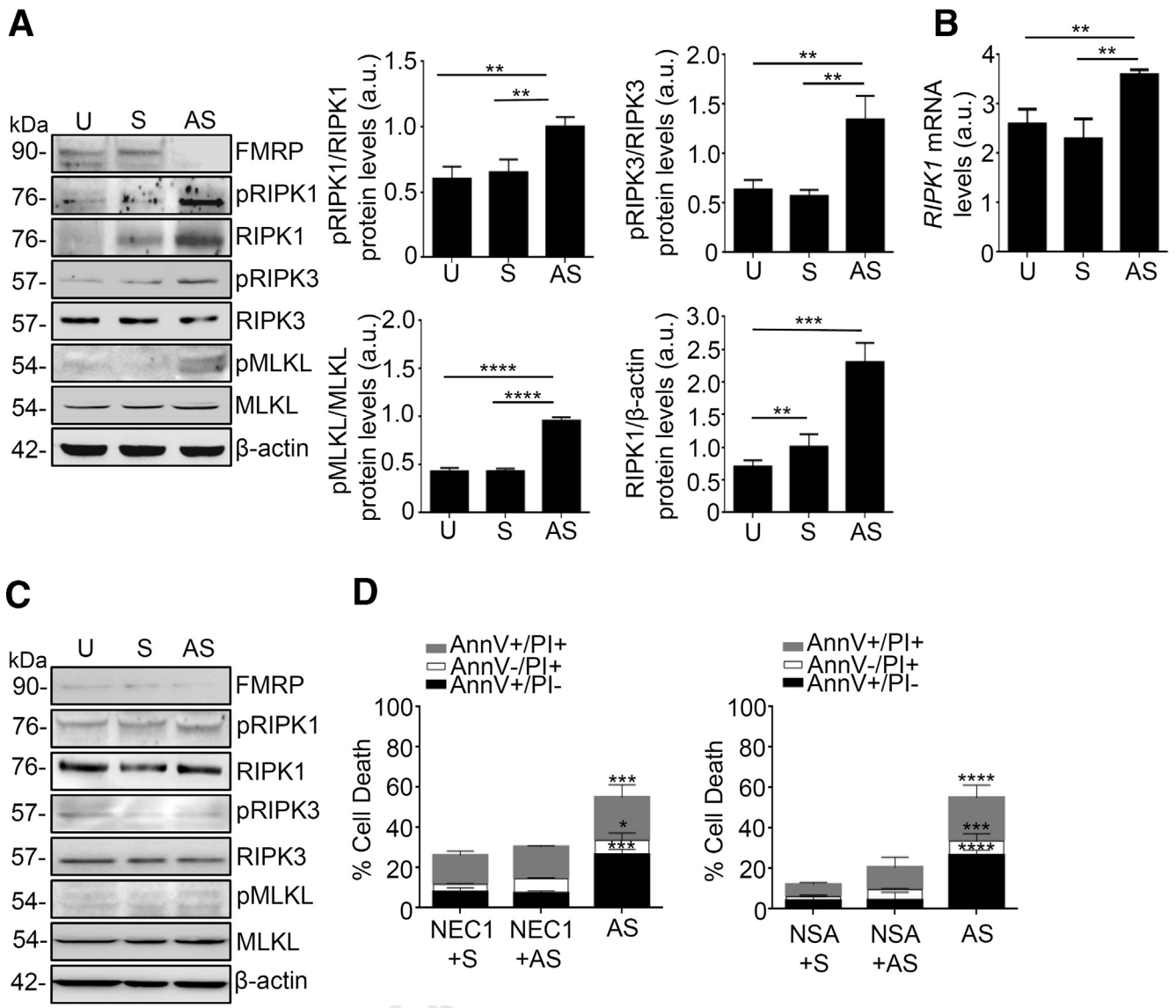

Figure 9. FMRP regulates the necroptotic pathway. (*A*) *Left*, representative Western blotting showing FMRP, pRIPK1, RIPK1, pRIPK3, RIPK3, pMLKL, MLKL, and β-actin in DLD-1 cells either untreated or treated with *FMR1* sense (S) or antisense (AS) oligonucleotide. *Right*, quantification of total pRIPK1, pRIPK3, pMLKL, and RIPK1 proteins in DLD-1 cells as measured by densitometry scanning of Western blotting (values are expressed in arbitrary units (a.u.), mean ± SD, n = 4; pRIPK1/RIPK1: U-cells and S-transfected cells versus AS-transfected cells, $^{**}P < .01$; pRIPK3/RIPK3: U-cells and S-transfected cells versus AS-transfected cells, $^{**}P < .01$; pMLKL/MLKL: β-actin, $^{****}P < .0001$; RIPK1/β-actin; U-cells and S-transfected cells versus AS-transfected cells, $^{**}P < .01$; $^{***}P < .001$). (*B*) *RIPK1* mRNA levels in DLD-1 cells untreated or treated with *FMR1* sense (S) or antisense (AS) oligonucleotide, normalized for *β-actin* (mean ± SD, n = 4; U-cells and S-transfected cells versus AS-transfected cells, $^{**}P < .01$). (*C*) Representative Western blotting showing FMRP, pRIPK1, RIPK1, pRIPK3, RIPK3, pMLKL, MLKL, and β-actin in HCEC-1ct cells unstimulated (U) or transfected with *FMR1* sense (S) or antisense (AS). (*D*) Percentage of AnnV and/or PI-positive DLD-1 cells pretreated with a specific RIPK1 inhibitor. *Left*, DLD-1 treated with RIPK1-specific inhibitor (NEC1). *Right*, human CRC cell lines treated with MLKL-specific inhibitor (NSA) and then transfected with *FMR1* sense (S) or antisense (AS) oligonucleotide (mean ± SD, n = 4; NEC1 plus S-transfected cells and NEC1 plus AS-transfected cells versus AS-transfected cells, $^{***}P < .001$; NSA plus S-transfected cells and NSA plus AS-transfected cells versus AS-transfected cells, $^{***}P < .001$, $^{****}P < .0001$). Statistical analysis of the data was performed using Student *t* test and Mann-Whitney test.

monitored for tumor formation and were endoscopically screened 1 week before being euthanized using a high-resolution endoscopic system. At week 22 after last AOM injection, mice were killed by cervical dislocation, and colonic tissues were collected for the different analyses. All experiments using animals were performed according to Italian and European legislation on animal experimentation (protocol number: 1138/2016-PR, 494/2017-PR).

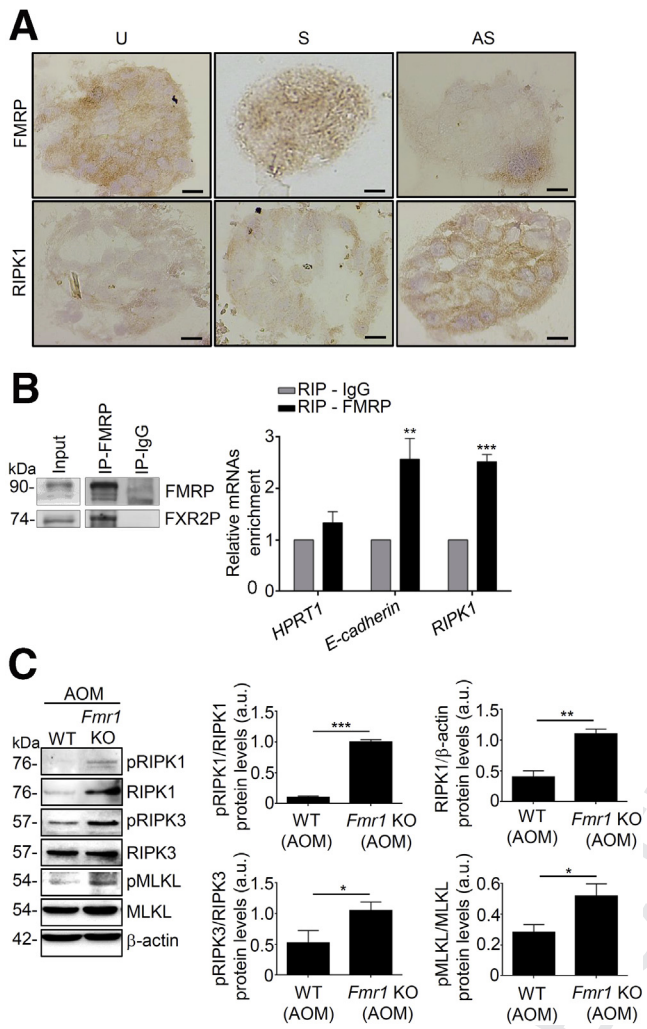

Figure 10. (*A*) Representative immunostaining images of FMRP (*upper panels*) and RIPK1 (*lower panels*) in human CRC organoids unstimulated (U) or transfected with sense (S) or *FMR1* antisense (AS) oligonucleotide, n = 2. (*B*) *Left*, representative Western blotting of FMRP immunoprecipitation from colon samples of 3 WT mice. FXR2P, a well-known FMRP interactor, is detected as part of the FMRP complex. Input (30 μg) of the total extract, FMRP immunoprecipitation (IP-FMRP), and mock immunoprecipitation (IP-IgG). *Right*, quantification by RT-qPCR of *Hprt1*, *E-cadherin,* and *RIPK1* mRNAs. *Hprt1* and *E-cadherin* mRNAs are negative and positive controls, respectively (mean ± SD, n = 3; *E-cadherin*: IP-IgG versus IP-FMRP, $^{**}P < .01$; *RIPK1*: IP-IgG versus IP-FMRP, $^{***}P < .001$). (*C*) *Left*, representative Western blotting showing pRIPK1, RIPK1, pRIPK3, RIPK3, pMLKL, MLKL, and β-actin in colon tissue of AOM WT and AOM *Fmr1* KO mice. *Right*, quantification of total pRIPK1, pRIPK3, pMLKL, and RIPK1 proteins in colon tissue AOM WT and AOM *Fmr1* KO mice as measured by densitometry scanning of Western blotting (values are expressed in arbitrary units (a.u.), mean ± SD of all experiments, n = 8 mice per group; $^{*}P < .05$, $^{**}P < .01$, $^{***}P < .001$). Statistical analysis of the data was performed using Student *t* test and Mann-Whitney test.

Mouse Endoscopy

Colonoscopy was performed blinded to the genotype by using the COLOVIEW (Karl Storz, Tuttlingen, Germany) high-resolution mouse endoscopic system.[57] The number of tumors was counted during endoscopic examination and performed at week 21 after the last AOM injection. All tumors were evaluated on the basis of their size and scored as previously described.[57] Tumors were graded as follows: grade 1 (very small but detectable tumor), grade 2 (tumor covering up to one-eighth of the colonic circumference), grade 3 (tumor covering up to one-fourth of the colonic circumference), grade 4 (tumor covering up to half of the colonic circumference), and grade 5 (tumor covering more than half of the colonic circumference).

Immunohistochemistry

All reagents were from Sigma-Aldrich (Milan, Italy) unless specified. Immunohistochemistry was performed on formalin-fixed, paraffin-embedded sections of normal tissues and tumoral samples of CRC patients. Sections were deparaffinized and dehydrated through xylene and ethanol, and the antigen retrieval was performed in Tris-EDTA citrate buffer (pH 7.8) for 30 minutes in a thermostatic bath at 98°C (Dako Agilent Technologies, Santa Clara, CA). Immunohistochemical staining was performed by using a monoclonal antibody directed against human FMRP (final dilution 1:5000; LifeSpan BioSciences, Seattle, WA) incubated at room temperature for 1 hour, followed by a biotin-free horseradish peroxidase (HRP) polymer detection technology with 3,3′diaminobenzidine as a chromogen MACH 4 Universal HRP-Polymer Kit (Biocare Medical, Pacheco, CA). Immunohistochemistry was performed on colonic cryosections of WT and *Fmr1* KO mice. The slides were incubated with a mouse monoclonal antibody directed against mouse Ki67 clone MIB-5, final dilution 1:100 (Dako, Agilent Technologies) at room temperature for 30 minutes, followed by biotin-free HRP polymer detection Ultravision Detection System (Thermo Scientific, Waltham, MA) with 3,3′diaminobenzidine as a chromogen (Dako, Agilent Technologies). Histopathologic analysis was performed on mouse colonic cryosections taken from WT and *Fmr1* KO mice in tumor and peritumor areas after H&E staining.

TUNEL Assay

In colonic cryosections taken from WT and *Fmr1* KO mice, TUNEL assay was performed to detect apoptotic cells using the in situ Cell Death Detection kit (Roche Applied Science, Penzberg, Germany) according to the manufacturer's instructions.

RNA Extraction, RT-PCR

RNA was extracted using PureLink mRNA mini kit (Thermo Fisher Scientific), according to the manufacturer's instructions. RNA (1 μg per sample) was reverse transcribed into complementary DNA (cDNA), and this was amplified using the following conditions: denaturation for 1 minute at 95°C; annealing for 30 seconds at 59°C for human *FMR1*; 60°C for human *CREB* and human/mouse *β-actin*; 61°C for human RIPK1, 30 seconds of extension at 72°C. Gene expression was calculated using the ΔΔCt formula.

A

Parameter	FMRP Immunoreactivity High	Low	p value
Grade Low grade High grade	14 (21%) 28 (42%)	11 (16%) 14 (21%)	**0,38**

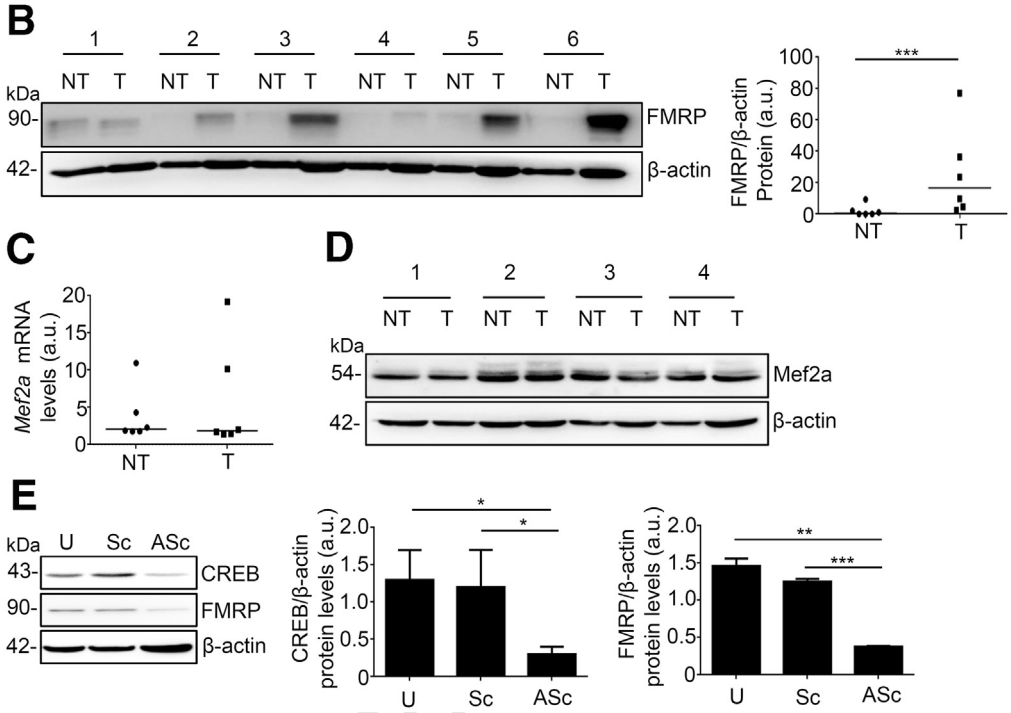

Figure 11. (*A*) Correlation between FMRP immunoreactivity and low or high risk of cancer progression in a cohort of human CRC (n = 67). Number of cases with weak-moderate FMRP or high FMRP expression and the percentage of FMRP-positive cases (%) are reported in each patient subgroup. Low grade is stage I/II, high grade is stage III/IV of CRC. (*B*) Total proteins extracted from both tumoral (T) and nontumoral (NT) areas of 6 patients with sporadic CRC were evaluated for FMRP expression by Western blotting. β-actin was used as loading control. *Right inset*, quantitative analysis of FMRP/β-actin protein ratio in total extracts of T and NT tissues taken from 6 patients with sporadic CRC, as measured by densitometry scanning of Western blots. Values are expressed in arbitrary units (a.u.) (***$P < .03$). (*C*) *Mef2* mRNA detected by RT-PCR and normalized to *β-actin* in colonic samples from 6 heathy subjects (NT) and tumoral areas (T) of 6 patients with sporadic CRC. (*D*) Representative Western blotting of Mef2 protein expression in paired colonic samples from 10 healthy subjects (NT) and 10 patients with sporadic CRC (T) (tumor areas). *Blots* are representative of 4 paired colonic samples. (*E*) *Left*, representative Western blotting of CREB levels in HCT-116 cells unstimulated (U) or transfected with *CREB* sense (Sc) or *CREB* antisense (ASc) oligonucleotide. *Right*, quantification of CREB/β-actin and FMRP/β-actin protein ratio (values are expressed in arbitrary units (a.u.), mean ± SD, n = 3; CREB/β-actin: U-cells and Sc-transfected cells versus ASc-transfected cells, *$P < .05$; FMRP/β-actin: U-cells and Sc-transfected cells versus CREB AS-transfected cells, **$P < .001$, ***$P < .01$). Statistical analysis of the data was performed using Student *t* test, Mann-Whitney test, and χ^2 test.

Sequences of the primer used were the following: human *FMR1* (forward 5′-GTTGAGCGGCCGAGTTTGTCAG-3′, reverse 5′-CCCACTGGGAGAGGATTATTTGGG-3′); human *CREB* (forward 5′-CCACTGATGGACAGCAGATC-3′, reverse 5′-CGGACCTCTCTCTTTCGTG-3′); human *RIPK1* (forward 5′-CACAAGGACCTGAAGCCTGAA-3′, reverse 5′-TGCTTGTTTTGAGCTGTAGCC-3′); human and mouse *β-actin* (forward 5′-AAGATGACCCAGATCATGTTTGAGACC-3′, reverse 5′-AGCCAGTCCAGACGCAGGAT-3′).

Protein Extraction and Western Blotting

Total proteins were extracted in buffer containing 10 mmol/L HEPES (pH 7.9), 10 mmol/L KCl, 0.1 mmol/L EDTA, 0.2 mmol/L ethylene glycol-bis (β-aminoethyl ether)-N,N,N′,N′-tetraacetic acid, and 0.5% Nonidet P40 supplemented with 1 mmol/L dithiothreitol, 10 mg/mL aprotinin, 10 mg/mL leupeptin, 1 mmol/L phenylmethylsulfonyl fluoride, 1 mmol/L Na3VO4, and 1 mmol/L NaF. Lysates were clarified by centrifugation and separated on sodium

dodecyl sulfate polyacrylamide gel electrophoresis. Membranes were incubated with antibodies against anti-human FMRP, CREB, MEF2a (Cell Signaling, Danvers, MA); pRIPK3, RIPK3, pMLKL, MLKL, RIPK1 (Abcam, Cambridge, UK); pRIPK1 (SAB, Maryland, WA) (final dilution 1:1000); anti-mouse FMRP, pRIPK3, RIPK3, pMLKL, MLKL, RIPK1 (Abcam); pRIPK1 (SAB), and PARP-1 (Cell Signaling), followed by a secondary antibody conjugated to HRP (Dako, Agilent Technologies). A mouse anti-β-actin antibody was used to detect β-actin and for normalization. A computer-assisted scanning densitometry was used to analyze the intensity of the immunoreactive bands.

Immunofluorescence

CRC cell lines and HCEC-1ct were fixed by 3.7% formaldehyde for 10 minutes at 4°C and permeabilized with 0.1% Triton for 10 minutes at room temperature, and nonspecific labeling was blocked (bovine serum albumin 1%, Tween 0.1%, glycine 2%) for 1 hour at room temperature. Anti-FMRP monoclonal antibody (1:500; Cell Signaling) was incubated overnight at 4°C. After washing with phosphate-buffered saline (PBS) 1 time, the secondary antibody goat anti-rabbit Alexa 488 (1:2000; Invitrogen, Carlsbad, CA) was applied for 1 hour at room temperature. Slides were washed with PBS 1 time, mounted using Prolong gold antifade reagent with DAPI (Invitrogen), and analyzed by a Leica DMI4000 B (Wetzlar, Germany) microscope with Leica application suite software (V4.6.2).

Flow Cytometry Analysis

Cells were untreated or transfected with either *FMR1* sense oligonucleotide (S) (final concentration 100 nmol/L) or *FMR1* antisense oligonucleotide (AS) (final concentration 0.5 nmol/L and 100 nmol/L) and were incubated with necrosulfonamide (final concentration 1μmol/L; Calbiochem, Milan, Italy) or necrostatin1 (final concentration 10 μmol/L; Cayman Chemical, Ann Arbor, MI). After 24 hours cells were collected, washed 2 times in AnnV buffer, stained with FITC-AnnV (final dilution 1:100; Immunotools, Friesoyte, Germany) according to the manufacturer's instructions, and incubated with 5 mg/mL PI for 30 minutes at 4°C. Cell death was quantified by flow cytometry; viable cells were considered as AnnV–/PI– cells.

Cells untreated or transfected with either *FMR1*S or *FMR1*AS oligonucleotide (final concentration 100 nmol/L) were incubated with Q-VD-OPh (final concentration 1μmol/L; R&D Systems, Minneapolis, MN). After 36 hours cells were collected, and caspase activation was quantified by flow cytometry using the specific antibody for cleaved caspase 3 and caspase 8 (final concentration 1:100; Biovision, Milpitas, CA). Staurosporin was used as apoptotic cell death positive control (final concentration 1 μmol/L; Sigma-Aldrich).

For cell cycle distribution, cells were left untreated or transfected with either *FMR1* S or *FMR1* AS oligonucleotide (final concentration 100 nmol/L). After 48 hours, cells were pulsed with 10 mol/L bromodeoxyuridine for 60 minutes, fixed in 70% cold ethanol, and stored at 20°C for at least 3 hours. Next, cells were denatured in 2 mol/L HCl and stained with anti–bromodeoxyuridine monoclonal antibody (Immunotech, Marseille, France), followed by fluorescein isothiocyanate–conjugated secondary anti-mouse immunoglobulin G (Molecular Probes, Milan, Italy). Cells were stained with 100 g/mL PI and analyzed by flow cytometry.

To assess mitochondrial membrane potential, we used JC-1 dye according to the manufacturer's instructions (Thermo Fisher Scientific).

Analysis was performed by using the Kaluza software (Beckman Coulter Life Sciences, Pasadena, CA).

Cell Culture, FMR1, and CREB Silencing

All reagents were from Sigma-Aldrich (Milan, Italy) unless otherwise specified. Human CRC cell line DLD-1 was obtained from the American Type Culture Collection (Manassas, VA) and cultured in RPMI 1640 and McCoy's 5A medium, respectively. All media were supplemented with 10% fetal bovine serum, 1% penicillin/streptomycin (both from Lonza, Verviers, Belgium). The healthy (normal) human colon epithelial cell line (HCEC-1ct) was obtained from EVERCYTE GmbH (Vienna, Austria) and cultured in ColoUp medium (EVERCYTE GmbH). Cells were maintained in a 37°C, 5% CO_2, fully humidified incubator. Phosphorothioate single-stranded oligonucleotide of the human *FMR1* complementary DNA sequence was synthesized in the antisense orientation (5′-TCCACCACCAGCTCCTCCAT-3′). CRC cell lines and HCEC-1ct were transfected with either *FMR1* antisense (AS) (final concentration 0.5–100 nmol/L) or *FMR1* sense (S) oligonucleotide (5′-AACACGTCTATACGC-3′, final concentration 100 nmol/L) for 24, 36, and 48 hours using Opti-MEM medium and lipofectamine 3000 reagent (both from Thermo Fisher Scientific) according to the manufacturer's instructions. CRC cell lines were transfected with either CREB antisense (ASc) (5′-GCATCTCCACTCTGCTGGTT-3′) or CREB sense (Ss) (5′-AACACGTCTATACGC-3′ at final concentration 200 nmol/L) for 24/48 hours.

Intestinal Crypt Isolation, Organoid Formation, and Immunostaining

Surgically resected intestinal tissues were obtained from colon cancer patients who underwent colon resection for sporadic CRC (all with TNM stages II–III) at the Tor Vergata University Hospital (Rome, Italy). Intestinal tissues were washed in Hanks' balanced salt solution (Lonza) containing 1% penicillin/streptomycin (Lonza) and chopped into approximately 5-mm pieces. Tissue fragments were placed in a tube, incubated in Advanced DMEM/F12 medium (Gibco, Monza, Italy) containing 15 mmol/L EDTA (Sigma-Aldrich), and rocked at 4°C for 30 minutes. Large chunks of tissue were then removed, and remaining crypts were centrifuged at 200*g* for 3 minutes, embedded in Matrigel (Becton Dickinson, Franklin Lakes, NJ), and seeded in warmed 48-well plates. Matrigel was allowed to solidify for 15 minutes at 37°C and overlaid with complete medium (advanced Dulbecco modified Eagle medium/F12 supplemented with 1% penicillin/streptomycin, 1% amphotericin B [Lonza], 0.1% gentamycin [Lonza], 1× B27 [Invitrogen],

HEPES [15 mmol/L; Lonza], 1× GlutaMAX-I [Gibco], rh-EGF [100 ng/mL; R&D Systems], rh-Noggin [100 ng/mL; R&D Systems], rh-R-Spondin [50 ng/mL; R&D Systems], and nicotinamide [10 mmol/L; Sigma-Aldrich]). The entire medium was replaced every 3 days. Organoids were transfected with either *FMR1* antisense (AS) (final concentration 200 nmol/L) or *FMR1* sense (S) oligonucleotide (final concentration 200 nmol/L) for 48 hours using Opti-MEM medium and lipofectamine 3000 reagent (both from Thermo Fisher Scientific) according to the manufacturer's instructions. Culture medium was removed, and organoids were washed with PBS and incubated with organoid harvesting solution (Trevigen, Winooski, VT) for 1 hour at 4°C with gentle shaking. Released organoids from depolymerized Matrigel were then collected and transferred into a Tissue-Tek Cryomold (Sakura Finetek Europe B.V., Alphen aan den Rijn, the Netherlands) containing optimal cutting temperature (OCT), frozen, and stored at −80°C. Immunohistochemical staining was performed using a monoclonal antibody directed against human RIPK1 (final dilution 1:250; Abcam), incubated at room temperature for 1 hour, followed by a biotin-free HRP-polymer detection technology with 3,3′diaminobenzidine as a chromogen MACH 4 Universal HRP-Polymer Kit (Biocare Medical). Sections were counterstained with hematoxylin, dehydrated, and mounted.

RNA Immunoprecipitation

All reagents were from Sigma-Aldrich unless specified. Human tumor samples, DLD-1 cells, and colon mouse tissues were lysed in ice-cold buffer (250 mmol/L NaCl, 20 mmol/L Tris/HCl pH 7.4, 10 mmol/L $MgCl_2$, 1% Triton X-100, 10 μL/mL protease inhibitor cocktail [Roche Applied Science, Penzberg, Germany], 10 μL/mL phosphatase inhibitor cocktails II and III, and 40 U/mL RNaseOUT [Invitrogen]). Dynabeads (Invitrogen) were incubated with a specific anti-FMRP antibody[58] or anti-rabbit immunoglobulin G (Santa Cruz Biotechnology, Santa Cruz, CA) in presence of 1% bovine serum albumin for 1 hour at room temperature. The beads were washed in wash buffer (250 mmol/L NaCl, 10 mmol/L Tris-HCl pH 7.4, 10 mmol/L $MgCl_2$, and 0.1% Triton X-100), and 800 μg of protein extract derived from 3 different human tumor samples, 800 μg of protein extract derived from DLD-1 cells, and 5 mg of protein extracts derived from colon tissues of 9 mice were added to the Dynabeads and incubated for 1–2 hours at 4°C. Proteins and RNA were eluted in Laemmli buffer and TRIzol, respectively. On immunoprecipitation, the co-immunoprecipitated RNA was extracted and analyzed by RT-qPCR using the StepOne Plus 7500 instrument (Life Technologies, Carlsbad, CA). Sequences of the primers used were the following: human *HPRT1* (forward 5′-TGCTGAGGATTTGGAAAGGGT-3′, reverse 5′-TCGAGCAAGACGTTCAGTCC-3′); human *β-actin* (forward 5′-ACCGAGCGCGGCTACAG-3′, reverse 5′-CTTAATGTCACGCACGATTTCC-3′); human *E-cadherin* (forward 5′-CGAGAGCTACACGTTCACGG-3′, reverse 5′-CTTTGTCGACCGGTGCAATC-3′); human *vimentin* (forward 5′-GCTTCAGAGAGAGGAAGCCG-3′, reverse 5′-AAGGTCAAGACGTGCCAGAG-3′); human *RIPK3* (forward 5′-CAGTGTGCAACAGGCAGAAC-3′, reverse 5′-TCAGTCCTTCTAAGCCGGGA-3′); human *RIPK1* (forward 5′-CACAAGGACCTGAAGCCTGAA-3′, reverse 5′-TGCTTGTTTTGAGCTGTAGCC-3′); mouse *Hprt1* (forward 5′-CAGCCCCAAAATGGTTAAGGTTGC-3′, reverse 5′-TCCAACAAAGTCTGGCCTGTATCC-3′); mouse *E-cadherin* (forward 5′-GTGACGCTGAAGTCCATGG-3′, reverse 5′-TTCAGAGGCAGGGTCGCG-3′); mouse *RIPK1* (forward 5′-GTCCACCGCCCGTCCT-3′, reverse 5′-GCTCAGAATCTCCAACACACC-3′).

Statistical Analysis

Values are expressed as mean ± standard deviation (SD) or ± standard error of the mean (SEM). Statistical analysis of the data was performed by using Student *t* test, Mann-Whitney test, or χ^2 test. GraphPad Prism 6 (GraphPad Software, La Jolla, CA) was used for statistical and graphical data evaluations. *P* values <.05 were considered statistically significant.

References

1. Jemal A, Bray F, Center MM, Ferlay J, Ward E, Forman D. Global cancer statistics. CA Cancer J Clin 2011; 61:69–90.
2. Hanahan D, Weinberg RA. Hallmarks of cancer: the next generation. Cell 2011;144:646–674.
3. Bisogno LS, Keene JD. RNA regulons in cancer and inflammation. Curr Opin Genet Dev 2018;48:97–103.
4. Parham LR, Williams PA, Chatterji P, Whelan KA, Hamilton KE. RNA regulons are essential in intestinal homeostasis. Am J Physiol Gastrointest Liver Physiol 2019;316:G197–G204.
5. Pereira B, Billaud M, Almeida R. RNA-binding proteins in cancer: old players and new actors. Trends in Cancer 2017;3:506–528.
6. Vo DT, Subramaniam D, Remke M, Burton TL, Uren PJ, Gelfond JA, de Sousa Abreu R, Burns SC, Qiao M, Suresh U, Korshunov A, Dubuc AM, Northcott PA, Smith AD, Pfister SM, Taylor MD, Janga SC, Anant S, Vogel C, Penalva LO. The RNA-binding protein Musashi1 affects medulloblastoma growth via a network of cancer-related genes and is an indicator of poor prognosis. Am J Pathol 2012;181:1762–1772.
7. Wurth L, Papasaikas P, Olmeda D, Bley N, Calvo GT, Guerrero S, Cerezo-Wallis D, Martinez-Useros J, Garcia-Fernandez M, Huttelmaier S, Soengas MS, Gebauer F. UNR/CSDE1 drives a post-transcriptional program to promote melanoma invasion and metastasis. Cancer Cell 2016;30:694–707.
8. Li Y, Tang Y, Ye L, Liu B, Liu K, Chen J, Xue Q. Establishment of a hepatocellular carcinoma cell line with unique metastatic characteristics through in vivo selection and screening for metastasis-related genes through cDNA microarray. J Cancer Res Clin Oncol 2003; 129:43–51.
9. Qie S, Majumder M, Mackiewicz K, Howley BV, Peterson YK, Howe PH, Palanisamy V, Diehl JA. Fbxo4-mediated degradation of Fxr1 suppresses tumorigenesis

in head and neck squamous cell carcinoma. Nature Communications 2017;8:1534.
10. Xing Z, Zeng M, Hu H, Zhang H, Hao Z, Long Y, Chen S, Su H, Yuan Z, Xu M, Chen J. Fragile X mental retardation protein promotes astrocytoma proliferation via the MEK/ERK signaling pathway. Oncotarget 2016; 7:75394–75406.
11. Bagni C, Tassone F, Neri G, Hagerman R. Fragile X syndrome: causes, diagnosis, mechanisms, and therapeutics. J Clin Invest 2012;122:4314–4322.
12. Bhogal B, Jepson JE, Savva YA, Pepper AS, Reenan RA, Jongens TA. Modulation of dADAR-dependent RNA editing by the Drosophila fragile X mental retardation protein. Nature Neurosci 2011;14:1517–1524.
13. Pasciuto E, Bagni C. SnapShot: FMRP mRNA targets and diseases. Cell 2014;158:1446–1446.e1.
14. Zalfa F, Panasiti V, Carotti S, Zingariello M, Perrone G, Sancillo L, Pacini L, Luciani F, Roberti V, D'Amico S, Coppola R, Abate SO, Rana RA, De Luca A, Fiers M, Melocchi V, Bianchi F, Farace MG, Achsel T, Marine JC, Morini S, Bagni C. The fragile X mental retardation protein regulates tumor invasiveness-related pathways in melanoma cells. Cell Death & Disease 2017;8:e3169.
15. Luca R, Averna M, Zalfa F, Vecchi M, Bianchi F, La Fata G, Del Nonno F, Nardacci R, Bianchi M, Nuciforo P, Munck S, Parrella P, Moura R, Signori E, Alston R, Kuchnio A, Farace MG, Fazio VM, Piacentini M, De Strooper B, Achsel T, Neri G, Neven P, Evans DG, Carmeliet P, Mazzone M, Bagni C. The fragile X protein binds mRNAs involved in cancer progression and modulates metastasis formation. EMBO Molecular Medicine 2013;5:1523–1536.
16. Schultz-Pedersen S, Hasle H, Olsen JH, Friedrich U. Evidence of decreased risk of cancer in individuals with fragile X. Am J Med Genet 2001;103:226–230.
17. Kalkunte R, Macarthur D, Morton R. Glioblastoma in a boy with fragile X: an unusual case of neuroprotection. Arch Dis Child 2007;92:795–796.
18. Wang H, Morishita Y, Miura D, Naranjo JR, Kida S, Zhuo M. Roles of CREB in the regulation of FMRP by group I metabotropic glutamate receptors in cingulate cortex. Molecular Brain 2012;5:27.
19. Bordonaro M, Lazarova DL. CREB-binding protein, p300, butyrate, and Wnt signaling in colorectal cancer. World J Gastroenterol 2015;21:8238–8248.
20. Di Giorgio E, Hancock WW, Brancolini C. MEF2 and the tumorigenic process, hic sunt leones. Biochimica et Biophysica Acta Reviews on Cancer 2018; 1870:261–273.
21. Smith KT, Nicholls RD, Reines D. The gene encoding the fragile X RNA-binding protein is controlled by nuclear respiratory factor 2 and the CREB family of transcription factors. Nucleic Acids Res 2006;34:1205–1215.
22. Hwu WL, Wang TR, Lee YM. FMR1 enhancer is regulated by cAMP through a cAMP-responsive element. DNA Cell Biol 1997;16:449–453.
23. Nambiar PR, Girnun G, Lillo NA, Guda K, Whiteley HE, Rosenberg DW. Preliminary analysis of azoxymethane induced colon tumors in inbred mice commonly used as transgenic/knockout progenitors. Int J Oncol 2003; 22:145–150.
24. Papanikolaou A, Wang QS, Papanikolaou D, Whiteley HE, Rosenberg DW. Sequential and morphological analyses of aberrant crypt foci formation in mice of differing susceptibility to azoxymethane-induced colon carcinogenesis. Carcinogenesis 2000;21:1567–1572.
25. Degterev A, Yuan J. Expansion and evolution of cell death programmes. Nat Rev Mol Cell Biol 2008; 9:378–390.
26. Danial NN, Korsmeyer SJ. Cell death: critical control points. Cell 2004;116:205–219.
27. Su Z, Yang Z, Xie L, DeWitt JP, Chen Y. Cancer therapy in the necroptosis era. Cell Death Differ 2016; 23:748–756.
28. He GW, Gunther C, Thonn V, Yu YQ, Martini E, Buchen B, Neurath MF, Sturzl M, Becker C. Regression of apoptosis-resistant colorectal tumors by induction of necroptosis in mice. J Exp Med 2017;214:1655–1662.
29. Gong Y, Fan Z, Luo G, Yang C, Huang Q, Fan K, Cheng H, Jin K, Ni Q, Yu X, Liu C. The role of necroptosis in cancer biology and therapy. Molecular Cancer 2019; 18:100.
30. Vanden Berghe T, Linkermann A, Jouan-Lanhouet S, Walczak H, Vandenabeele P. Regulated necrosis: the expanding network of non-apoptotic cell death pathways. Nat Rev Mol Cell Biol 2014;15:135–147.
31. Linkermann A, Green DR. Necroptosis. N Engl J Med 2014;370:455–465.
32. van der Flier LG, Clevers H. Stem cells, self-renewal, and differentiation in the intestinal epithelium. Annu Rev Physiol 2009;71:241–260.
33. Fearon ER. Molecular genetics of colorectal cancer. Annu Rev Pathol 2011;6:479–507.
34. Waldner MJ, Neurath MF. The molecular therapy of colorectal cancer. Molecular Aspects of Medicine 2010; 31:171–178.
35. Chatterji P, Rustgi AK. RNA binding proteins in intestinal epithelial biology and colorectal cancer. Trends Mol Med 2018;24:490–506.
36. Wurth L, Gebauer F. RNA-binding proteins, multifaceted translational regulators in cancer. Biochim Biophys Acta 2015;1849:881–886.
37. Legrand N, Dixon DA, Sobolewski C. AU-rich element-binding proteins in colorectal cancer. World Journal of Gastrointestinal Oncology 2019;11:71–90.
38. Schwemmle S, de Graaff E, Deissler H, Glaser D, Wohrle D, Kennerknecht I, Just W, Oostra BA, Doerfler W, Vogel W, Steinbach P. Characterization of FMR1 promoter elements by in vivo-footprinting analysis. Am J Hum Genet 1997;60:1354–1362.
39. Evan GI, Vousden KH. Proliferation, cell cycle and apoptosis in cancer. Nature 2001;411:342–348.
40. Lowe SW, Cepero E, Evan G. Intrinsic tumour suppression. Nature 2004;432:307–315.
41. Ascano M Jr, Mukherjee N, Bandaru P, Miller JB, Nusbaum JD, Corcoran DL, Langlois C, Munschauer M, Dewell S, Hafner M, Williams Z, Ohler U, Tuschl T. FMRP targets distinct mRNA sequence elements to regulate protein expression. Nature 2012;492:382–386.

42. Darnell JC, Van Driesche SJ, Zhang C, Hung KY, Mele A, Fraser CE, Stone EF, Chen C, Fak JJ, Chi SW, Licatalosi DD, Richter JD, Darnell RB. FMRP stalls ribosomal translocation on mRNAs linked to synaptic function and autism. Cell 2011;146:247–261.
43. Miyashiro KY, Beckel-Mitchener A, Purk TP, Becker KG, Barret T, Liu L, Carbonetto S, Weiler IJ, Greenough WT, Eberwine J. RNA cargoes associating with FMRP reveal deficits in cellular functioning in Fmr1 null mice. Neuron 2003;37:417–431.
44. Sawicka K, Hale CR, Park CY, Fak JJ, Gresack JE, Van Driesche SJ, Kang JJ, Darnell JC, Darnell RB. FMRP has a cell-type-specific role in CA1 pyramidal neurons to regulate autism-related transcripts and circadian memory. eLife 2019;8.
45. Di Marino D, Achsel T, Lacoux C, Falconi M, Bagni C. Molecular dynamics simulations show how the FMRP Ile304Asn mutation destabilizes the KH2 domain structure and affects its function. J Biomol Struct Dyn 2014; 32:337–350.
46. Darnell JC, Jensen KB, Jin P, Brown V, Warren ST, Darnell RB. Fragile X mental retardation protein targets G quartet mRNAs important for neuronal function. Cell 2001;107:489–499.
47. Bagni C, Zukin RS. A synaptic perspective of fragile X syndrome and autism spectrum disorders. Neuron 2019; 101:1070–1088.
48. Garant JM, Perreault JP, Scott MS. G4RNA screener web server: user focused interface for RNA G-quadruplex prediction. Biochimie 2018;151:115–118.
49. Doluca O. G4Catchall: a G-quadruplex prediction approach considering atypical features. J Theor Biol 2019;463:92–98.
50. Zhuang Y, Xu HC, Shinde PV, Warfsmann J, Vasilevska J, Sundaram B, Behnke K, Huang J, Hoell JI, Borkhardt A, Pfeffer K, Taha MS, Herebian D, Mayatepek E, Brenner D, Ahmadian MR, Keitel V, Wieczorek D, Haussinger D, Pandyra AA, Lang KS, Lang PA. Fragile X mental retardation protein protects against tumour necrosis factor-mediated cell death and liver injury. Gut 2020;69:133–145.
51. Feng X, Song Q, Yu A, Tang H, Peng Z, Wang X. Receptor-interacting protein kinase 3 is a predictor of survival and plays a tumor suppressive role in colorectal cancer. Neoplasma 2015;62:592–601.
52. Moriwaki K, Bertin J, Gough PJ, Orlowski GM, Chan FK. Differential roles of RIPK1 and RIPK3 in TNF-induced necroptosis and chemotherapeutic agent-induced cell death. Cell Death & Disease 2015; 6:e1636.
53. Han W, Li L, Qiu S, Lu Q, Pan Q, Gu Y, Luo J, Hu X. Shikonin circumvents cancer drug resistance by induction of a necroptotic death. Mol Cancer Ther 2007; 6:1641–1649.
54. Steinhart L, Belz K, Fulda S. Smac mimetic and demethylating agents synergistically trigger cell death in acute myeloid leukemia cells and overcome apoptosis resistance by inducing necroptosis. Cell Death & Disease 2013;4:e802.
55. Meurette O, Rebillard A, Huc L, Le Moigne G, Merino D, Micheau O, Lagadic-Gossmann D, Dimanche-Boitrel MT. TRAIL induces receptor-interacting protein 1-dependent and caspase-dependent necrosis-like cell death under acidic extracellular conditions. Cancer Res 2007;67:218–226.
56. Basit F, Cristofanon S, Fulda S. Obatoclax (GX15-070) triggers necroptosis by promoting the assembly of the necrosome on autophagosomal membranes. Cell Death Differ 2013;20:1161–1173.
57. Stolfi C, Rizzo A, Franze E, Rotondi A, Fantini MC, Sarra M, Caruso R, Monteleone I, Sileri P, Franceschilli L, Caprioli F, Ferrero S, MacDonald TT, Pallone F, Monteleone G. Involvement of interleukin-21 in the regulation of colitis-associated colon cancer. J Exp Med 2011;208:2279–2290.
58. Ferrari F, Mercaldo V, Piccoli G, Sala C, Cannata S, Achsel T, Bagni C. The fragile X mental retardation protein-RNP granules show an mGluR-dependent localization in the post-synaptic spines. Mol Cell Neurosci 2007;34:343–354.

Received February 13, 2020. Accepted October 16, 2020.

Correspondence
Address correspondence to: Ivan Monteleone, MD, PhD, Department of Biomedicine and Prevention, University of Rome "Tor Vergata", Via Montpellier 1, 00133 Rome, Italy. e-mail: ivan.monteleone@uniroma2.it; fax: •••; or Claudia Bagni, PhD, Department of Fundamental Neurosciences, University of Lausanne, Lausanne, Switzerland and Department of Biomedicine and Prevention, University of Rome "Tor Vergata", Via Montpellier 1, 00133 Rome, Italy. e-mail: claudia.bagni@uniroma2.it.

Acknowledgments Q4
The authors thank Vittoria Mariano for her help in making the graphical abstract using Adobe Illustrator and thank Laura Pacini and Maria Giulia Farace for advice and guidance. Q19

CRediT Authorship Contributions
Antonio Di Grazia (Data curation: Lead; Investigation: Lead; Methodology: Lead; Visualization: Lead; Writing – original draft: Lead)
Irene Marafini (Data curation: Equal; Formal analysis: Equal; Methodology: Equal; Writing – review & editing: Equal),
Giorgia Pedini (Data curation: Equal; Formal analysis: Equal; Writing – review & editing: Equal)
Davide Di Fusco (Data curation: Equal; Formal analysis: Equal; Writing – review & editing: Equal)
Federica Laudisi (Data curation: Equal; Formal analysis: Equal)
Vincenzo Dinallo (Data curation: Equal; Formal analysis: Equal)
Eleonora Rosina (Data curation: Equal; Formal analysis: Equal)
Carmine Stolfi (Data curation: Equal; Formal analysis: Equal)
Eleonora Franzè (Data curation: Equal; Formal analysis: Equal)
Pierpaolo Sileri (Data curation: Supporting)
Giuseppe Sica (Data curation: Supporting)
Giovanni Monteleone (Funding acquisition: Supporting; Methodology: Supporting; Writing – review & editing: Supporting),
Claudia Bagni (Conceptualization: Equal; Formal analysis: Equal; Methodology: Equal; Supervision: Equal; Writing – original draft: Equal; Writing – review & editing: Equal),
Ivan Monteleone (Conceptualization: Lead; Data curation: Equal; Formal analysis: Lead; Funding acquisition: Equal; Investigation: Lead; Methodology: Lead; Supervision: Lead; Writing – original draft: Lead; Writing – review & editing: Lead)

Conflicts of interest
The authors disclose no conflicts. Q5

Funding
Supported by the following funds: Associazione Italiana Sindrome X Fragile, Telethon GGP15257, and Etat de Vaud to CB and by Nogra Pharma Ltd (Dublin, Ireland) to IMo. The funders had no role in study design, data analysis, decision to publish, or preparation of the manuscript. Q6